# SELECTIVE TOUGHENING OF CARBON/EPOXY COMPOSITES USING GRAPHENE OXIDE

By

SESHASAI GANDIKOTA

Bachelor of Engineering in Mechanical Engineering

Osmania University

Hyderabad, India

2008

Submitted to the Faculty of the
Graduate College of the
Oklahoma State University
in partial fulfillment of
the requirements for
the Degree of
MASTER OF SCIENCE
December, 201

SELECTIVE TOUGHENING OF CARBON/EPOXY

COMPOSITES USING GRAPHENE OXIDE

Thesis Approved:

Dr. Jay C. Hanan

Thesis Adviser

Dr. Ranji Vaidyanathan

Dr. Raman P. Singh

Dr. Sheryl A. Tucker

Dean of the Graduate College

TABLE OF CONTENTS

# LIST OF TABLES

Table Page

# LIST OF FIGURES

Figure Page

# CHAPTER I

# INTRODUCTION

Composites are increasingly replacing metals in the industry and are materials of choice in various applications due to their outstanding strength to weight ratios and thermo-mechanical properties [1].

Epoxy resins, being the building blocks of widely used composite combinations, are evolving as materials of focus for polymer chemists to address the performance needs of industry. Tons of epoxy resins and their respective hardeners are produced every year and increasing number of formulations of the same are being introduced at the same time. A recent forecast by the industrial analysts estimates global epoxy resins market to reach 1.93 Million Tons by 2015 [2]. Aerospace industry holds a key share in these markets and is seeking more resin formulations with better performance capabilities.

## 1.1 Epoxy Resins

Epoxy resins are a family of thermosetting polymers characterized by two or more oxirane (epoxide groups) rings within their monomer configurations [3]. These rings can participate in a variety of reactions forming cross-linked compounds, attributing to their versatile structural applicability. These resins when cured, form materials suitable for structural applications with

variety of reactions forming cross-linked compounds, attributing to their versatile structural applicability. . Figure 1 shows the structure of an epoxide ring.

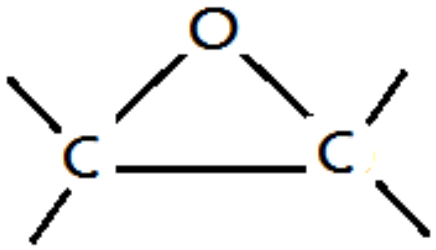


**Figure 1: Epoxide ring**

On the negative side, these resin systems suffer low toughness values and it is believed that the brittleness can be related to their high cross-linking, which makes the molecular motion difficult. This results in low energy absorption during fracture and hence lower fracture toughness [4]. The problem can be overcome by optimizing the process parameters like the layup sequence, curing time and processing technique. Thus toughening of polymers is a topic of high interest and different approaches are being evaluated and introduced to resolve the issues. Use of secondary phase fillers is among some of the popular methods of toughening. Due to the ease of processing, secondary phase fillers have a variety of advantages over conventional processing methods. Also, in the commercial applications and developments standpoint, secondary reinforcement of polymers is one of the easiest ways to achieve properties not available in individual materials.

One common secondary type of fillers for epoxy systems are the carbon based nanoparticles like the carbon nanotubes (CNTs), fullerenes (Bucky balls) and graphene nanoparticles [5]. Among all the nano-forms of carbon family, there has been an increased interest in the use of graphene as secondary phase filler material due to its exceptional mechanical, thermal, electrical and barrier properties.

## 1.2 Graphene nanoparticles

Graphene is a single 2-D layer of graphite with a hexagonal array of carbon atoms in which each atom is bonded to three of its neighboring atoms [6]. It is naturally available in the form of graphite, which is a stack of several graphene sheets held together by weak Vander Wall's forces. These layers possess large surface areas and surface energies. The bonding type in graphene (sp2 carbon-carbon) being the strongest type of bonding (theoretically), gives graphene its extraordinary structural properties.

Graphene oxide, otherwise called graphitic acid, is an oxide form of graphite that still preserves the parental layer-like structure and terminated by oxygen rich groups like epoxide, carbonyl and hydroxyl. Because of the availability of both hydrophilic and hydrophobic (basal planes) groups, graphene oxide is an amphiphilic compound and its affinity for water attributes to its high dispersibility in it. Figure 2 is the expected structure of graphene oxide.

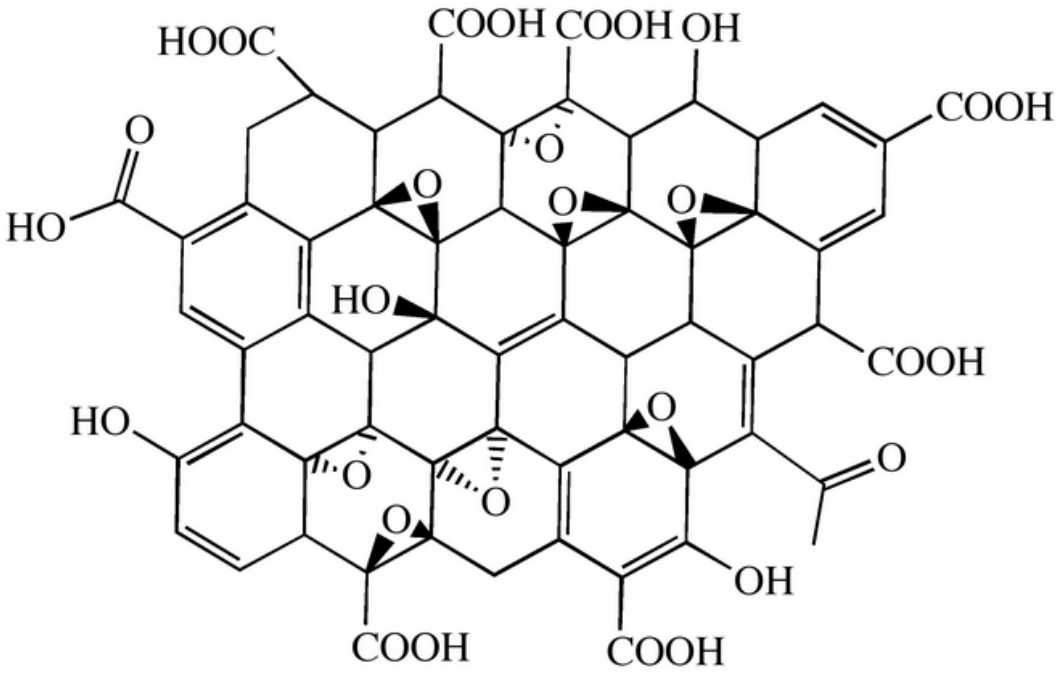


**Figure 2: Expected structure of graphene oxide [7]**

## 1.3 Overview of the study

The present work focuses on the enhancement of toughness properties of carbon fiber reinforced plastics (CFRPs) using graphene oxide nanofillers. The effect of graphene oxide dispersed in polyvinyl Pyrrollidone (PVP) solution and incorporated into the interface of the composite laminates will be studied. According to the current hypothesis, the propagating crack in the composites is deflected (tilting and twisting) in the presence of graphene oxide, resulting in fracture toughness improvement in the composites. Double cantilever beam (DCB) testing will be employed to estimate the energy absorbed in delaminating the laminates. A comparison of energy required for fracture, varying graphene oxide content will be brought to optimize the graphene oxide content. Also, the effect of graphene oxide particles on the application temperatures (glass-transition temperatures) of the composites will be studied, at different doping levels. Detailed characterization of the fracture surface will be done to understand the mechanisms involved in the toughening process.

Scanning electron microscopy (SEM) studies will be performed to look at the nano-structure of un-exfoliated and exfoliated graphene oxide. TEM analysis is also performed to examine the structure of graphene oxide layers. Three point bending tests will be performed on the composites for measuring the flexural properties.

# CHAPTER II

## HYPOTHESIS

Contemporary polymer composite materials used are polymers filled with high strength fibers in the direction in which properties are desired. As a result, continuity of fiber does not exist in the through thickness direction. This discontinuous characteristic of these laminates results in structural weakness [8] (low interlaminar strength) and leads to delamination fracture.

The basic modes of fracture in laminated composites can be categorized into three classes based on the type of loading in the matrix. They are opening mode (Mode I), sliding mode (Mode II) tearing mode (Mode III) [9]. Figure 3 shows the typical modes of failure in composites.

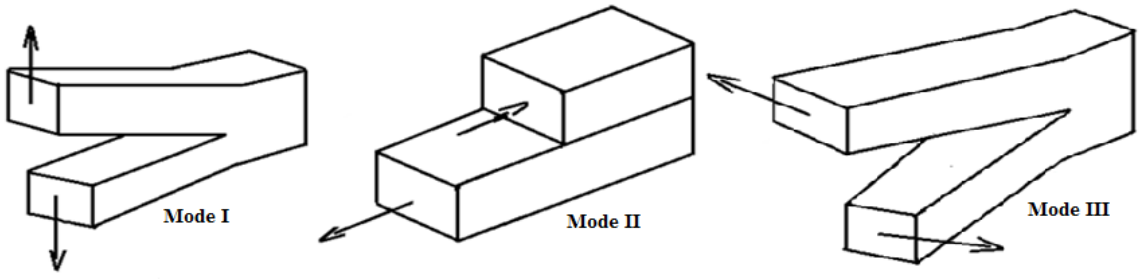


**Figure 3: Typical modes of fracture observed in composites**

There is already enough understanding that the energy required to propagate mode I type of crack is the least compared to other types. Trakas et al. have measured the strain energy release rates for the three basic modes with varying stacking designs [10] on carbon-fiber/epoxy laminates.

The results in in the paper have been shown in Figure 4: Comparison of fracture toughness values in different modes Figure 4. From the plot, it is clear that the energy required for mode I delamination is significantly low compared to modes II and III. It can further be inferred that the composites are more susceptible to mode I fracture than others and that there is a need to improve the mode I fracture toughness for improved structural performance.

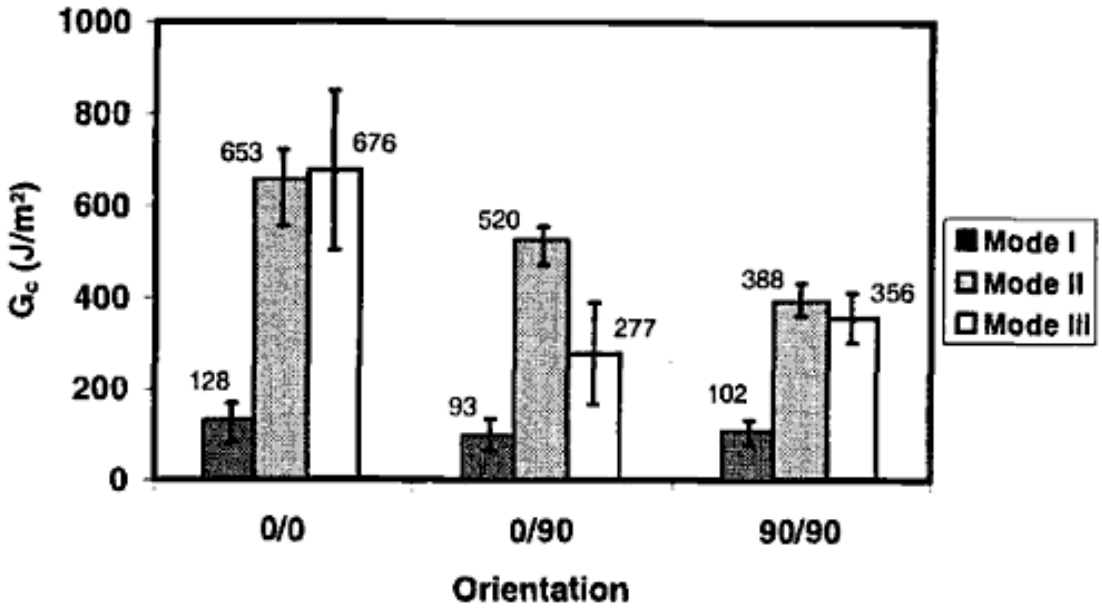


**Figure 4: Comparison of fracture toughness values in different modes [10]**

Also, efforts have been put to improve the mode I fracture toughness in these composites using various nanofillers through bulk modification [11-13]. This involves usage of high amounts of nanofillers, resulting in increased material cost.

The main aim in the current study is to improve the fracture toughness of polymer composite laminates with the use of minimal amount of nanofillers in the interfaces. To achieve the goal of locally incorporating nanofillers into the composite laminates, Polyvinyl Pyrrolidone, a thermosetting polymer compatible with epoxy systems [14] is proposed as a carrier for the

nanoparticles. The polymer apart from acting as a carrier and compatibilizer, is expected to perform a variety of roles including interacting in between the graphene plates.

According to the proposed hypothesis, graphene oxide plates could act as deflectors in path of a propagating crack in interlaminar region and deviate it from its original direction. Consequently, fracture surface area could increase and thereby the work of fracture in mode I opening improved. This argument is also supported by literature available on plate like nanofillers [15, 16]. Research available on the use of plate like nanofillers like clay, graphene and molybdenum disulfide showed improvement in mechanical properties [17-21]. Also, functionalization of graphene by chemical oxidation is expected to modify the surface energy and enhance interfacial bonding with epoxy resin.

The use of graphene oxide in polymer composite systems for improvement of mode I interlaminar has not been explored yet and the results are expected to be a good contribution to the scientific society.

### 2.1 Choice of graphene oxide

Studies reveal that two-dimensional graphene sheets as nanofillers have higher efficiency to resist fracture and fatigue than one-dimensional carbon nanotubes [17]. These properties can be attributed to the high aspect ratios of graphene sheets. Also, it has been shown that graphene has a strong affinity to form hydrogen bonding with water, which is an added advantage to its exfoliation and dispersion in aqueous solutions [22].

The choice of graphene oxide is made because of its potential to interact chemically with various resin systems, while physically enhancing the properties like a filler material. The presence of functional groups like carboxylic, epoxide, ketone and carbonyl result in its high compatibility with epoxy and other resin systems, making it a suitable filler material for the improvement of

mechanical properties. The carboxylic groups present in graphene oxide are expected to involve in addition reactions while other functional groups involve in hydrogen bonding. Given the versatile applications of epoxies in structural systems, graphene oxide nanoparticles incorporated into epoxies are expected to manifest themselves as practical solutions for high performance composite materials.

The major hurdle in the process is isolation of graphene oxide plates and their incorporation into the polymer hosts. The problem is addressed by the use of an ultrasonicator, which creates shockwaves in the medium that are capable of exfoliation. Also, a low viscosity polymer like Polyvinyl Pyrrolidone (PVP) that can form films and compatible with the epoxy systems is used to intercalate between the graphene oxide plates and to act as a carrier of the nanoparticles. The choice of the carrier polymer is critical in the process because its existence in the interface is as significant as the matrix material and can influence the interface properties directly.

### 2.2 Role of Polyvinyl Pyrrolidone

The major role of PVP in composites is to be a polymer carrier for nano-fillers into the interlaminar region. Also, PVP is a potential material to stabilize nanoparticles, especially graphene compounds [23]. Outstanding crosslinking properties of PVP and its compatibility with most of the polymers [24] make it a suitable material for the current technique. M. Munz et al. in the book "Adhesion – Current Research and Application" studied an epoxy formulation sandwitching a PVP film. It was reported that PVP acts as a good compatibilizer for epoxy systems, improving the mechanical properties of the resin. The mechanism of PVP – GO interacting with resin system can be predicted as absorption and adsorption [25] (in this process, chemical reaction). High absorption activity is observed in epoxy/PVP interfaces, accompanied by some adsorption [25]. The extent of absorption or adsorption of epoxy molecules into films depend on mobility of PVP molecules in the curing process. The mobility can be varied by

controlling pressure and temperature conditions in the curing process. Mobility is further dependent on glass transition temperature of PVP, thereby on its molecular weight [14] thus PVP K60, which has a moderate glass-transition temperature (around the composite curing temperature), is used. Oyama et al. in "Interdiffusion at the Interface between Poly (vinylpyrrolidone) and Epoxy" studied epoxy/PVP interface and reported strong chemical interactions between epoxy and the carbonyl functional group of PVP [14].

Other rational behind using PVP is its potential as an intercalant. There is literature available on the use of PVP as an intercalant in case of plate like nanoparticles (montmorillonite clay) [26-28]. Also, PVP has proved to be a good stabilizer for nanoparticles like gold, CNTs and graphene [23, 29]. Physical association of PVP with CNTs has been shown to enhance the dispersion of CNT in both water and organic solvents [30]. The possible mechanism for the interaction of polymer solvents with nanoparticles is by wrapping. Figure 5: Proposed combining mode of graphene oxide – PVP/Epoxy compositespresents a schematic of proposed reaction between graphene oxide, PVP, epoxy and the amine.

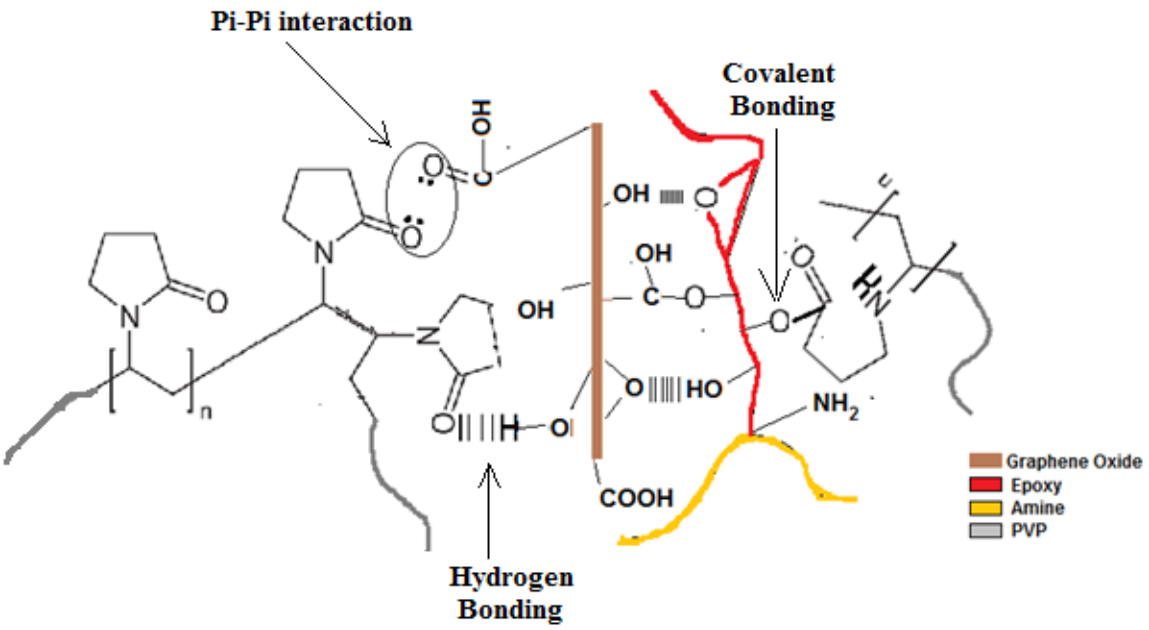


**Figure 5: Proposed combining mode of graphene oxide – PVP/Epoxy composites**

### 2.3 Selective toughening

The mechanism of toughening associated with the current method of applying nanoparticles in between laminas is to present increased local resistance to a propagating crack in the interface. In other words, our aim is to slow down crack propagation by introducing mechanically dissimilar obstacles in the most probable delamination path.

As opening mode or mode I type of fracture takes the minimum energy [31] (among the basic modes) to cause composite failure, improving mode I toughness properties is of interest. Moreover, toughening is needed only in the interlaminar region and not in the bulk. The method employed in this study involves selective toughening of composites in the interlaminar region only. Painting of PVP dispersed nanofillers is expected to improve the interlaminar fracture toughness in composites.

Jenny Win et al. applied a similar method to ceramic composites by using very thin alumina interlayers coated with alumina slurry in a polymer. The composites obtained displayed high

mechanical properties [32]. Figure 6 describes the concept of fracture toughness enhancement using fillers in the interface. It can be understood from the schematic that we expect an increase in the crack length, leading to higher energy absorption.

Similar attempt by Wang et al. to incorporate silicon carbide whiskers in the interface yielded a 50% increase in the fracture toughness [33]. Yuan Li et al. incorporated vapor grown carbon nanofibers into carbon fiber reinforced composites in the interlayer and observed a 25% improvement in the fracture toughness with an addition of vapour grown carbon fibers in the interface (about 12.7 wt % in the entire sample) [34]. Masahiro Arai et al. incorporated vapour grown carbon nanofiber in the interlaminar region and achieved a 50% improvement in the fracture toughness with about 7-13 volume percent of filler composition.

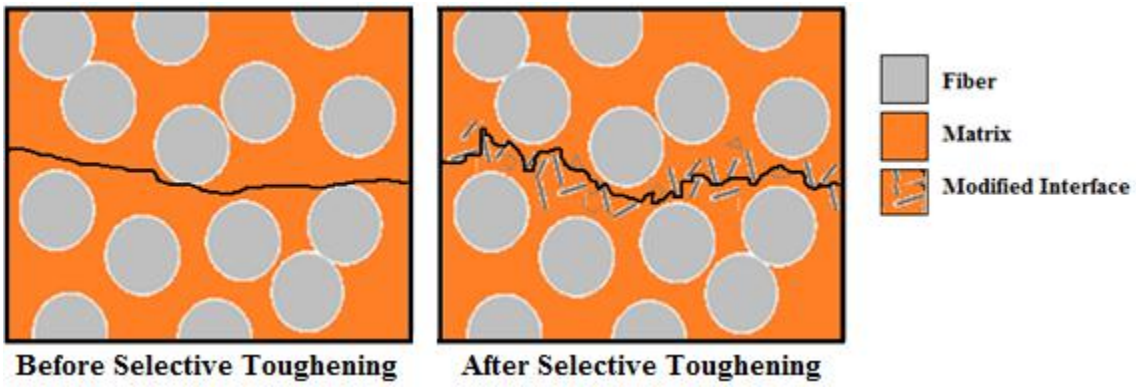


**Figure 6: Schematic of selective toughening**

The effect of interlaminar toughening using graphene oxide on mode I fracture toughness is quantified using double cantilever method and the values are compared to check if the hypothesis is true. Also, fractography studies can give a clear understanding of the mechanisms of toughening.

# CHAPTER III

# BACKGROUND REVIEW

Polymer nanocomposites have been using nanofillers like carbon black, carbon nanotubes, and layered silicates for enhancement of mechanical, thermal, electrical, and other properties [28, 35, 36]. The discovery of graphene as a new member of the carbon allotropes family lead to a new class of modified polymer materials with enhanced properties.

## 3.1 History of Graphene

Graphite and its oxide forms have a history that dates back to some of the earliest studies on the chemistry of graphite [37]. Brodie, a British chemist in 1859 put efforts to oxidize graphite in the presence of nitric acid and potassium chlorate. He named the oxide obtained as "graphic acid". The oxide form was easily dispersible in pure water and not dispersible in acids. Staudenmaier in 1898 improved the method by using concentrated sulfuric acid as well as fuming nitric acid. The change in the procedure resulted in highly oxidized graphene oxide.

The next significant contribution to the graphite oxide chemistry was by Hummers and Offeman, who developed an alternative method to oxidize graphite by treating it with a mixture of potassium permanganate ($KMnO_4$) and concentrated sulfuric acid ($H_2SO_4$) [38]. Though there is research on the use of these nanoparticles in various nanocomposites, efforts to obtain free standing one atom thick layers remained unsuccessful till a recent work on free standing graphene layers got a Nobel Prize for physics in 2011.

### 3.2 Structure and properties of graphene compounds

Graphite is a member of the allotrope family of carbon. Its structure can ideally be described as consisting of layers of hexagonally arranged carbon atoms covalently bound to three other carbon atoms. These in-plane carbon – carbon covalent bonds are formed through sp2-sp2 orbital overlap and thus possess highest bond strength while, across the planes, the layers are held together by weak Vander Waals forces. The unsymmetrical bonding style observed is because all the valance electrons are used up to form σ and π bonds among the carbons in the in-plane direction [39]. As a result, graphite has superior properties in the in-plane direction compared to out-of-plane direction. Figure 7: crystal structure of graphite shows the atomic arrangement in the graphite crystal lattice.

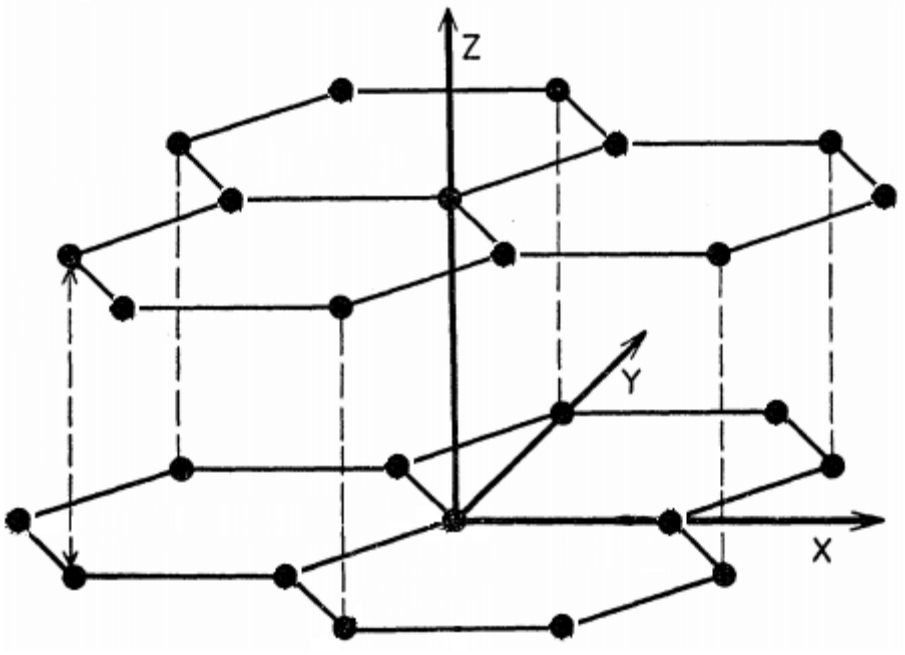


**Figure 7: crystal structure of graphite [40]**

Graphene is a term used for an exfoliated form of graphite. In other words, the plates in graphite are well separated. The mechanical properties of single graphene reported show that it is the strongest material ever tested. According to the measurements, graphene has a tensile strength of 130GPa and elastic modulus of 1 TPa [41].

These properties pose it as a benchmark for structural and mechanical applications. Table 1 shows a comparison between moduli of various materials.

**Table 1: Comparison of young's moduli of different materials [42]**

| Material | Young's modulus (E) in GPa |
|---|---|
| Rubber (small strain) | 0.01 – 0.1 |
| PTFE (Teflon) | 0.5 |
| Nylon | 3 – 7 |
| Oak wood (along grain) | 11 |
| Concrete(under compression) | 30 |
| Aluminum alloy | 69 |
| Glass | 65 – 90 |
| Titanium (Ti) | 105 – 120 |
| Copper (Cu) | 110 – 130 |
| Silicon (S) | 150 |
| Wrought iron and steel | 190 – 210 |
| Tungsten (W) | 400 – 410 |
| Silicon carbide (SiC) | 450 |
| Diamond (C) | 1,050 – 1200 |
| Single walled carbon nanotube | 1000 |
| Graphite/Graphene | 1000 |

Graphite oxide is also a plate like structure with functionalized organic groups attached to the edges of the plates. It preserves the parental structural properties and exhibits better chemical reactivity due to the presence of organo functional groups like the epoxide, carboxylic, carbonyl and ketone, which make it reactive with a variety of polymer systems [43].

**Table 2: Pricing and availability of Graphene Oxide and other nano-additives**

| | POSS | Dendrites | Hyperbranched Polymers | Diamond Adamantane | Fullerenes | Carbon MWNT | Graphene | Graphene Oxide |
|---|---|---|---|---|---|---|---|---|
| **Available Amounts** | 100s of Tons | Kilograms | Kilograms | Tons | Kilograms | 100s of Tons | 100s of Tons | 100s of Tons |
| **Price($/Kg)** | 10s | 100s | 10s | 100s | 1000s | 1000s | 100s | 10s |
| **Solubility** | Good | Good | Good | Good | Poor | None | None | Good |
| **Diversity of Chemistries** | Very Good | Good | Good | Poor | Fair | Poor | Good | Very Good |
| **Aspect ratio** | Good | Good | High | Good | High | High | Very High | Very High |

### 3.3 Exfoliation and intercalation of graphene plates

Considering the fact that lower dimensionalities of graphite show enhanced reactivity, it is desirable to have the graphene oxide layers separated improve the reactivity with the resin system. The process of separation is sometimes termed as exfoliation or intercalation. Exfoliation is a concept of randomizing the particles in the compound resulting in an increase in the surface area and thus volume. In terms of graphene and its oxides, exfoliation is the process of randomizing and separation of plates, resulting in a more disoriented system. In this process, there will be an expansion in the z axis direction resulting in a material with a reduction in density. On the other side, intercalation is a widely studied way of separating graphite plates using layers of intervening atoms or molecules resulting in compounds with isolated graphene layers embedded in a 3D matrix.

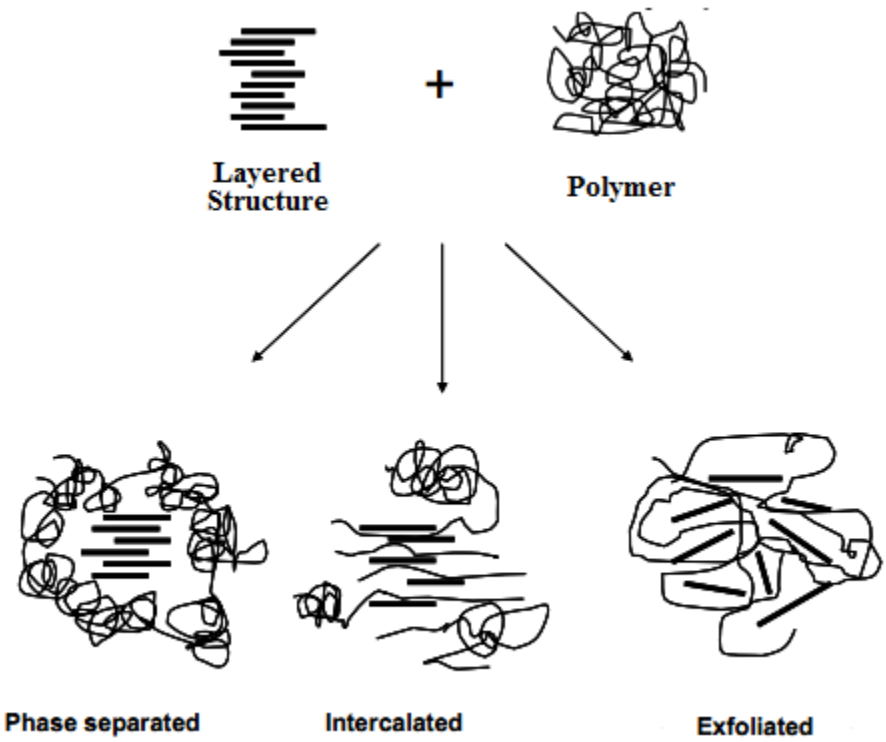


**Figure 8: Exfoliation and Intercalation in plate like materials**

Chemical, thermal and physical methods have been well explored in isolation of graphene plates and the 2 D crystals have been characterized [44-46] and these methods result in exfoliation and/or intercalation of layered structures [47-50]. Figure 8: Exfoliation and Intercalation in plate like materials shows a schematic of the process of exfoliation and intercalation in layered structures.

Theorists like Landau and Peierls in their work on two-dimensional crystal lattices predicted that existence of lower dimensions is thermodynamically unstable and could not exist [51]. The thermal fluctuations in low-dimensional crystal lattices may lead to atomic displacements comparable to interatomic distances and may finally result in their instability [52]. Also, the melting point of materials rapidly decreases with decreasing thickness (around atomic scale) and this may result in decomposition into few atoms. With this argument, atomic monolayers are being grown as an integral part of larger 3D structures. This process of growing monolayers epitaxially continued until the experimental discovery of graphene and other free-standing 2D atomic crystals.

The discovery lead to the Nobel Prize for physics 2011. The thermal fluctuation problem in the case of 2D graphene is overcome by the sp2 hybridized carbon bonding (strongest type of bonding) and thus the atomic vibrations are minimal. The extracted 2D crystals of graphene becomes intrinsically stable by small crumpling in the third dimension leading to a gain in elastic energy and reduces the effect of thermal vibrations.

### 3.4 Toughening of polymers using nanofillers

Toughening of polymers has been an area of research through years because of their intrinsic brittle properties [53-57]. The basic theme of toughening of polymers is to improve their crack resistance (fracture toughness) without decreasing other properties [58]. Several attempts have been made to tailor the properties of polymers to the needs using a variety of nano fillers with

different interaction mechanisms. The nature of interaction of these fillers could be either physical, chemical or a combination of both [59].

Physical interaction is a process where the mechanical properties are enhanced when the fillers physically interact to increase the resistance of deformation. This can be looked at as a nanocomposite with fillers as reinforcement, transferring load to the matrix. The physical interaction is dependent on the shape of the filler and its aspect ratio.

Some of the commonly used physically interacting fillers are carbon nanotubes, fullerenes, clay, graphene, thermoplastics, graphite and others [55, 60, 61]. The degree of property enhancement is a function of various parameters like the dimensionality of the filler, composition, modulus mismatch between the matrix and filler and dispersion. For example, Wang and his colleagues invested the effect of clay on the mechanical properties of epoxy nanocomposites [18]. They observed an improvement in both Young's modulus and fracture toughness at a clay percentage of 2.5 by weight of epoxy. Rafiee studied fullerene modified epoxies and reported a 20% enhancement of ultimate tensile strength compared to the baseline epoxy polymer with 0.5% of fullerenes. A fracture energy study on the same polymer demonstrated a 93% improvement in fracture toughness (Kic) with 1% nanofillers over pristine epoxy [62].

In chemical interaction mechanisms, the fillers chemically react with the polymer domains and either completely of partially modify the properties of the polymer. Examples of chemically interacting nanofillers include graphene oxide, functionalized carbon nanotubes, polyhedral Oligomeric Silsesquioxanes (POSS) and several others [63-65]. These fillers form chemical bonds with the matrix that improve the material properties. The degree of improvement depends on the type of bonds that are formed. Covalent bonds being the most favorite, hydrogen bonding, pi-pi interactions and other types of bonding make the molecular motion difficult and thereby improve the properties.

Kelkar studied mode I fracture toughness in glass fiber reinforced composites by incorporation alumina nanoparticles [66] and achieved a 51% increase in the Mode I fracture toughness values. However, functionalization of these nanoparticles produced a 74% improvement. Yadav et. al. tried interleaving of Kevlar fibers in the interface of carbon/epoxy composites. An improvement of 100% in fracture toughness was observed with a 6% reduction of flexural modulus [67].

Research on use of chemically interacting nanofillers has also seen success in improving the mechanical properties [60]. Moniruzzaman investigated on a method to graft single wall nanotubes to epoxy systems. Grafting improved flexural modulus by 17% and flexural strength by 10% over neat resin with about 0.05% by weight of nanotubes. A similar approach by Liu et al. using chemically functionalized carbon nanotubes demonstrated a 78% improvement in the tensile modulus with 0.8 wt% of functionalized nanotubes [68]. Use of a variety of POSS nanofillers in the resin systems in structural composites resulted in significant improvement in thermo-mechanical properties [69].

### 3.5 Graphene and graphene oxide as nanofillers

Graphene oxide is a class of nanofiller that can interact both chemically as well as physically. The basal planes help crack deflection and the functional groups at the edges help modifying the resin. Given these advantages and the fact that the individual plates of graphene oxide can be isolated, graphene and its oxide form are looked at as potential fillers for the enhancement of thermal, mechanical and electrical properties [70].

Min et al. worked on the improvement of toughness and dielectric properties of epoxy resins using graphite nanosheets [71]. They observed that the dielectric constant of epoxy/graphite nanosheet composites improved with 3.5 wt% graphite filler content. They also achieved a 35% improvement in storage modulus, toughness and tensile properties. Rafiee et al. explored the possibility of graphene oxide as nanofillers for fracture toughness improvement and other properties. They used thermally exfoliated graphene oxide to modify epoxy resins in the bulk and

observed significant improvement in the toughness, stiffness, flexural strength, and fatigue resistance at lower nanofiller loading fractions [17].

Zaman et al. conducted similar study on two types of epoxies with functionalized graphene. They exfoliated graphene using sonication and chemically modified to obtain functionalization. They observed a 96% improvement of fracture energy release rate at 4 wt% graphene concentration. Also, an improvement in glass transition temperature was observed at 2.5 wt% [72].

Graphene oxide is also looked at in biomedical industry as a form of reinforcement. Xiaoming et al. used graphene oxide as a nano-reinforcement in chitosan matrix. They observed an improvement of 122% in tensile modulus and 64% in Young's modulus with about 1 wt % of graphene oxide [73]. Also, Hailong et al. looked at the biocompatibility of graphene oxide reinforced chitosan nanocomposites and observed improvement in modulus [74].

### 3.6 Toughening mechanism in graphene filled composites

Several toughening mechanisms have been proposed with the use of nanofillers and have been thoroughly studied in literature [53, 55, 58, 75, 76]. Secondary phase nanoparticles located near the tip of a propagating crack disturb the crack front, causing a reduction in stress intensity. Some of the very common toughening mechanisms observed in carbon-fiber/Epoxy composites are crack bowing, crack deflection, fiber bridging and plastic deformation. Among these mechanisms, crack bowing and crack deflection are a simultaneously occurring phenomenon. The first produces a nonlinear crack (can be in the same plane) while the second produces non-planar crack [15, 16].

#### 3.6.1 Crack Deflection

Deflection toughening is a phenomenon where a propagating crack in a matrix material will change its course when obstructed by a filler material. Faber and Evans in "Crack deflection processes I and II" describe the mechanism of crack deflection [15, 16, 76]. A propagating crack on encountering an obstacle will deflect into a different plane due to a drop in stress concentration

at the crack tip, either by tilting or twisting. As the energy required to fail the composite in mode II or mode III stress states is higher compared to mode I failure, there will be an improvement in fracture toughness. The fracture toughness improvement can also be related to an increase in fracture surface area due to the torturous path laid down by the fillers due to crack deflection. The deflection process makes the crack path torturous and increases the fracture surface area, leading to higher energy absorption. The deflection is caused by the elastic modulus and/or thermal expansion mismatch between the matrix and the particulate phase. The sign of the residual strain determines the direction of the deflection[76, 77].

### 3.6.2 Crack Bowing

Crack pinning or bowing occurs due to the resistance of secondary phase particles to the propagating crack in the matrix. In this condition, the crack tends to bow between the particles resulting in reduction of stress intensity along the length of the bowed crack [78]. Also, the length of the crack increases and thereby the fracture toughness. The stress intensity at the particle-matrix interface increases till the fracture toughness of the particle is reached and then the crack propagates further. Figure 9 shows the schematic of crack bowing mechanism observed in nanocomposites.

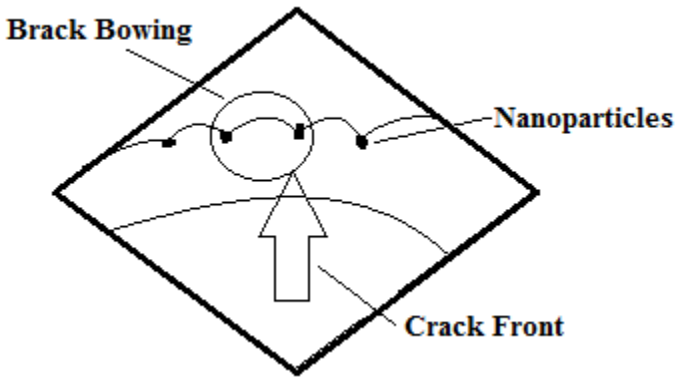


**Figure 9: Crack pinning mechanism**

Bernd Wetzel et al. studied the fracture and toughening mechanisms in epoxy resins containing titanium dioxide ($TiO_2$) or aluminum oxide ($Al_2O_3$) [78]. They observed significant crack pinning on the fracture surface.

Rutnakornpituk discussed the possible mechanism of toughening of thermoplastic filled thermosetting polymers [55]. He proposed that the role of thermoplastic particles is to behave as impenetrable objects for the crack and slow down the rate of crack propagation.

### 3.6.3 Crack Bridging

Crack bridging is a process of toughening where the fibers restrict the relative displacement between the opposite crack faces and thus slow delamination growth by decreasing the local stress intensity at the tip of the delamination. The fillers in the composite span two crack surfaces and alleviate the stress required for further propagation of crack. Figure 10 shows a schematic that depicts the fiber bridging process of toughening.

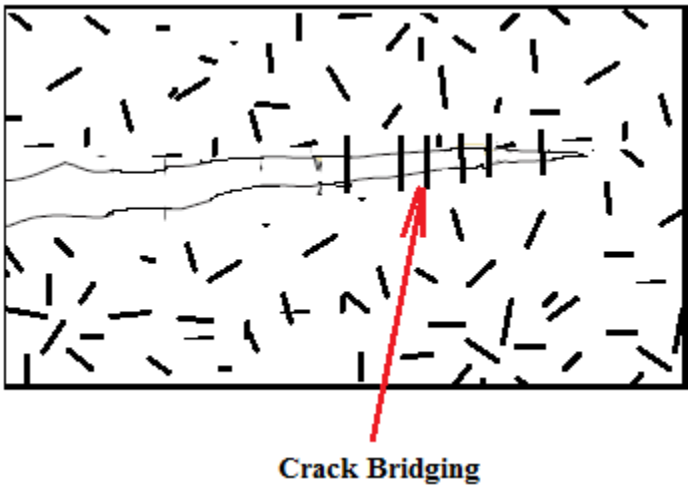


**Figure 10: Crack bridging mechanism**

Rutnakornpituk while discussing about the mechanism of toughening using thermoplastics, proposed the possibility of the thermoplastic materials phase separating and spanning the crack surfaces [55].

Spearing et al. investigated the effect of fiber bridging in composites on the fracture toughness of the composites [79]. They observed that interlaminar fracture resistance is sensitive to fiber bridging.

### 3.6.4 Plastic Deformation

Plastic deformation mechanism of toughening is a phenomenon in which the matrix acquires the required energy to flow in front of the crack tip, thereby blunting the tip. The flow results in localized shear yielding and plastic flow in the material adjacent to the fracture surfaces and thereby absorbing more energy before propagation of crack.

The plastic flow can be improved by suspending nanoparticles throughout the matrix [80]. McGarry et al. compared the chemical bond energy to the fracture energy of toughened epoxy resin systems. They observed a difference between measured and calculated values of bond breakage energy due to localized shear yielding and plastic flow in the material near the fracture surface.

# CHAPTER IV

# MATERIALS AND TESTING

The present chapter focuses on the materials used, the sample making procedure and characterization procedures involved in the process. Graphene oxide is incorporated into the interlaminar region by dispersing it in polyvinyl Pyrrollidone and painting it in the interface. Specimens are prepared varying the graphene oxide content in the PVP solution. Improvement in properties of composites due to the embedded graphene oxide plates is studied through various experiments and characterization techniques.

## 4.1 Graphene oxide

The graphene oxide required for the investigation was prepared following a protocol by Marcano et. al, "Improved synthesis of Graphene oxide" [81]. The process is a modification of Hummers' process [38]. In the hummers' process, graphite oxide is obtained by oxidizing graphite using agents like sulfuric acid, sodium nitrate and potassium permanganate. The reaction between sulfuric acid and potassium permanganate produces manganese heptoxide, a highly volatile compound dark green in color. Manganese heptoxide further dissociates into manganese dioxide and ozone.

In the Hummers' process, flake graphite was initially added to sodium nitrate and suspended in sulfuric acid in a container maintained at 0 $^{o}$ C. Calculated amount of potassium permanganate is added to the suspension while agitating to complete the oxidation process.

The method currently followed uses phosphoric acid along with the sulfuric acid to increase the amount of oxidation. Expanded graphite (1 weight equivalent) was suspended in a 9:1 mixture of concentrated sulfuric acid and phosphoric acid. Potassium permanganate (6 weight equivalents) was added to the solution and the reaction mixture was stirred for 12 hours. Water was added to the solution and stirred to obtain a brown dispersion. The obtained solution was then filtered to obtain a brown paste, which is graphite oxide with some bi-products as impurities (mostly manganese dioxide). The obtained paste was suspended in water and centrifuged at 4000 rpm for 1hour to obtain graphene oxide separated from the solution. The process of centrifugation was iterated five to six times and finally dispersed in ethanol. The obtained solution was washed in succession with 200 ml of water, 200 mL of 30% hydrochloric acid, and 200 ml of ethanol. The final brown solid obtained had lot of water and was then dried at room temperature to obtain graphite oxide. Washing with HCl is to dissolve manganese oxide and separate it from the solution. Figure 11 shows the graphene oxide dispersed in water.

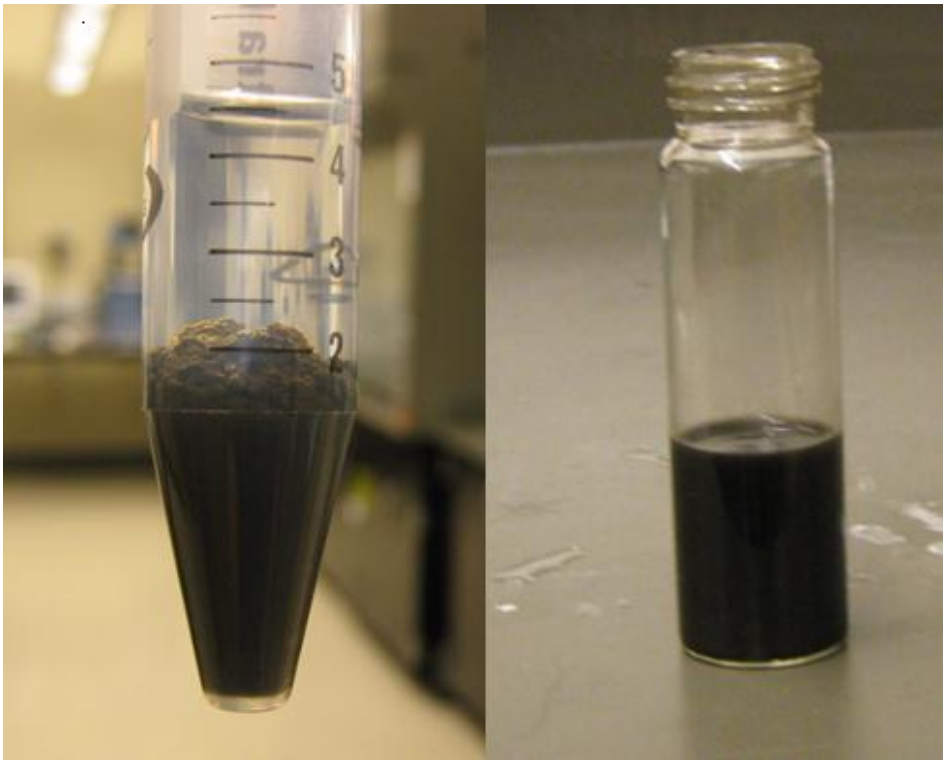


**Figure 11: Graphene oxide dispersion in water**

### 4.2 Exfoliation of graphene oxide

The oxidized form of graphite obtained was dispersed in polyvinyl Pyrrolidone (PVP) expecting intercalation of PVP chains in the inter-planar regions of graphene sheets. A Qsonica's S-4000 type ultrasonicator with a 0.5 inch probe was used to exfoliate the graphene oxide plates.

Ultrasonicator is a device that converts electrical signal into physical vibration that can be utilized to agitate a solution. It consists of a probe that vibrates at a very high frequency, nucleating cavities in the solution. Cavitation occurs when a series of pockets of space between the molecules are formed and collapsed. Several such bubbles forming and collapsing continually create powerful waves of vibration that cycle into the solution and separate apart the plates, intercalating or exfoliating the nanoparticles. Figure 12 shows 1% by weight of graphene oxide nanoparticles dispersed in poly vinyl Pyrrollidone using an ultrasonic probe.

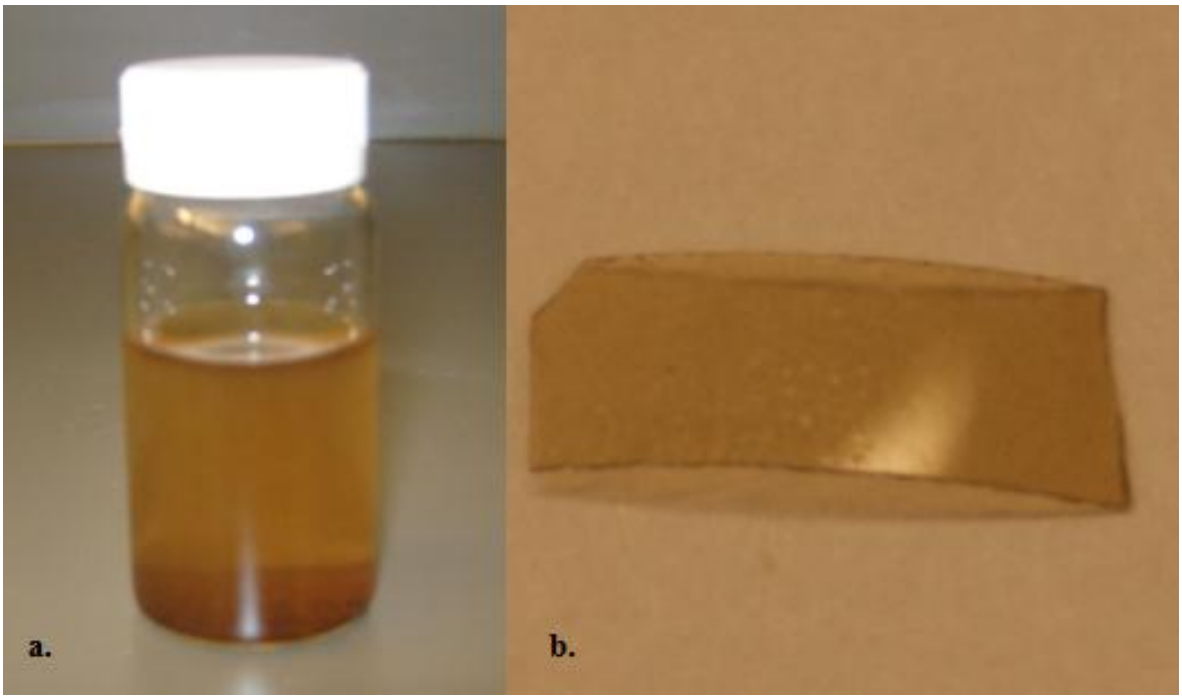


**Figure 12: (a.) 1 % GO – PVP solution (b.) 1% GOES – PVP film**

### 4.3 Characterization of graphene oxide

The graphene oxide powder obtained by the process has been characterized using two equipment. X-ray diffraction analysis was done to check the diffraction pattern in the material. X-ray diffraction patterns were collected in reflection, on a Bruker D8 Discovery diffractometer, using Cu Kα laser (λ = 1.54054 Å) radiation. A small amount of the graphene oxide powder on a clean glass slide was characterized using a Cu Kα laser. The same procedure was carried out on the starting material graphite. The intensity of the light diffracted at different diffraction angles was recorded and the intensity versus 2ɵ plots for graphene oxide and graphite are compared. Also, the d-spacing in the nanofillers is calculated and compared using Braggs law. The basic principle of Bragg's law is shown in Figure 13: Bragg's law. The governing equation for diffraction of light is given as

$$n\lambda = 2d \sin\theta \quad (1)$$

Where

**λ** = wavelength of the x-ray

**θ** = scattering angle

**n** = integer representing the order of the diffraction peak.

**d** = inter-plane distance of (i.e atoms, ions, molecules)

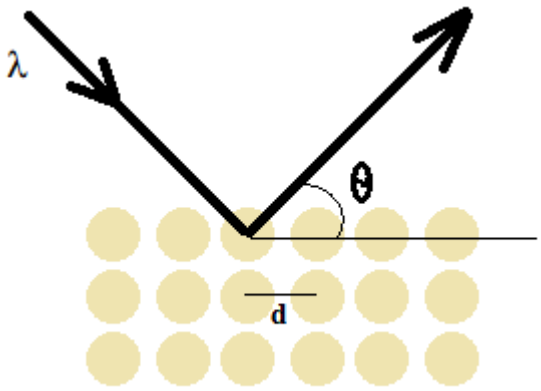


**Figure 13: Bragg's law**

The unexfoliated and exfoliated versions of graphene oxide were looked at in a Hitachi S-4800 SEM Scanning electron microscope (SEM). The specimen in the study being nonconductive, have been coated with gold (upto 50 nm thick, 1 minute exposure) using a crissington sputter coater before microscopy. Intercalated graphene oxide has been observed in the a transmission electron microscope to understand the dispersion.

### 4.4 Composite panel fabrication

Composite laminates were prepared for studying the effect of graphene oxide in the interface. Three types of samples, for double cantilever beam (DCB) testing, flexure testing and dynamic mechanical analysis were fabricated for the current study.

The basic process for making composite laminates involved the use of pre-impregnated carbon fabric obtained from TCR composites. The prepreg obtained was a C105-3K- Plain Weave fabric pre-impregnated by a phenolic novalac based resin (36% resin). Sixteen layers of prepregs were cut according to the planned dimensions and exfoliated graphene oxide in PVP solution was painted on the surface. The coated prepregs were allowed to dry at room temperature for half an hour and stacked in order. Sufficient care was taken while stacking to maintain the 0-0 layup sequence in the samples to avoid the possible effect of the layup design parameters on the fracture

toughness. The stacked prepregs were cured using a hot-press that can apply uniform pressure all through the sample. The curing cycle followed was according to the manufacturer's specifications. The samples were ramped up at less than $5^0$ F/min till $310^0$ F and held for 1 hour. They were then cooled down to at least $150^0$ F before removing from the hot-press at less than $5^0$ F/min ramp-down rate. Figure 14 shows a composite laminate prepared using this method.

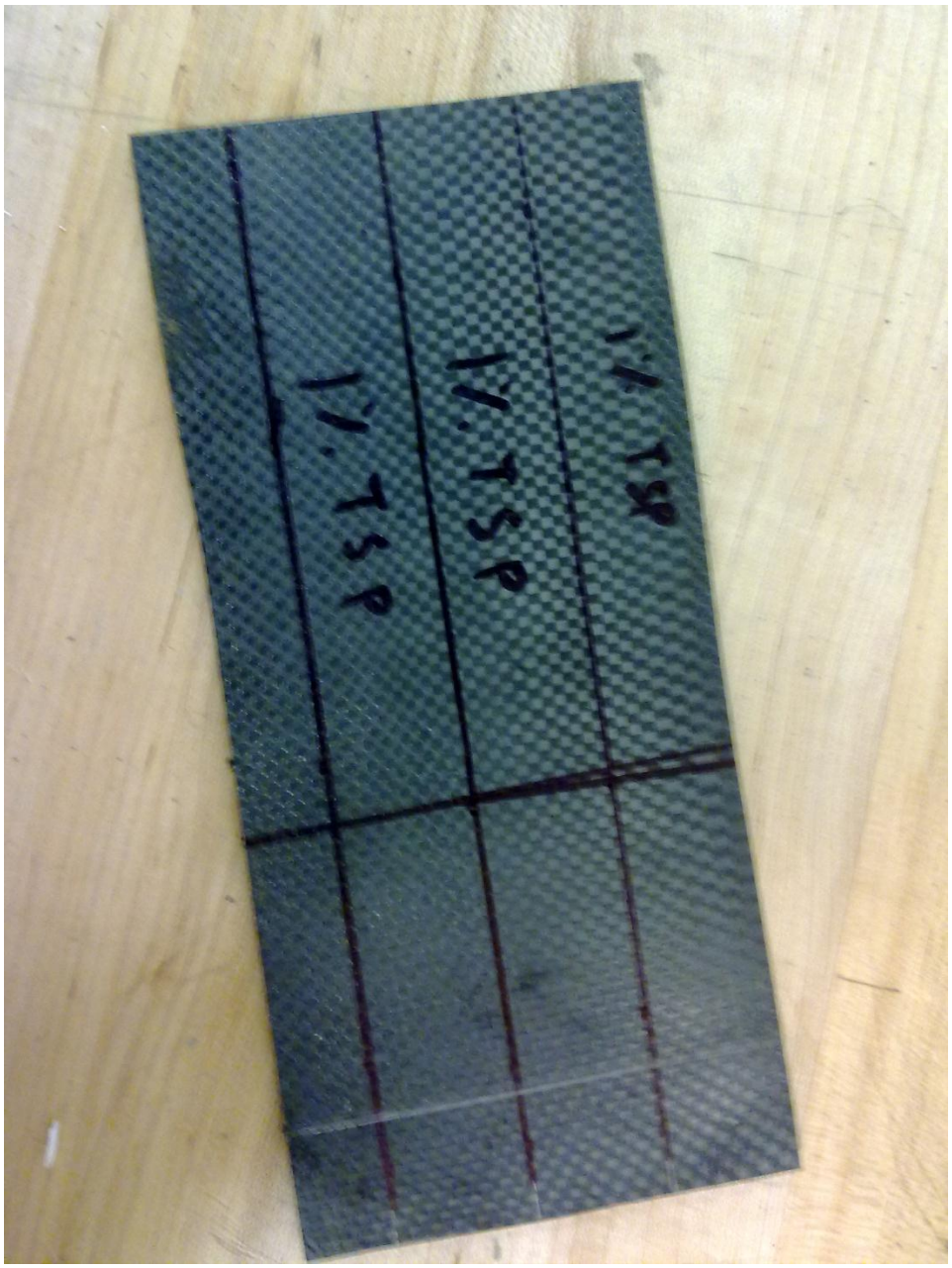


**Figure 14: Composite laminate**

Samples with only PVP and no nanofiller were used as control and the effect of filler was studied varying the level of doping. Samples were cut according to the ASTM sample dimensions for mode I fracture toughness measurement, flexure testing and dynamic mechanical analysis.

### 4.5 Fracture toughness measurement

The mode I fracture toughness of the composite plies was measured using an instron machine according to the ASTM standard D 5528 [82]. The process of testing involved introduction of known length of crack in the samples and measuring the energy required for failing the samples in mode I fracture. Samples were made by painting the nanoparticles dispersed in PVP solution in the mid-plane of the 16 layered prepreg stack and then curing them. A non-adhesive Teflon (PTFE) insert, 13 μm thick was introduced at the mid-plane of the laminate during layup to form an initial crack.

A pair of piano hinges were bonded to the end of each specimen to transfer the load to the sample. The hinge tabs were selected such that they can sustain the load operated in the testing process. The distance from the loading block pin to the center line of the top specimen arm was kept as small as possible to minimize the errors resulting from the applied moment arm during the testing.

The bonding surfaces were lightly scrubbed with sandpaper and wiped clean with acetone to avoid possible contamination before bonding. A cyanoacrylate based glue (superglue) was used to adhere the surfaces together and allowed to dry. The edge of the specimen was painted using a liquid ink corrector (of low viscosity) to ease the visual detection of crack propagation. The painted edge was graduated in millimeters to facilitate easy measurement of the crack length. Figure 15 shows a schematic of a typical DCB sample.

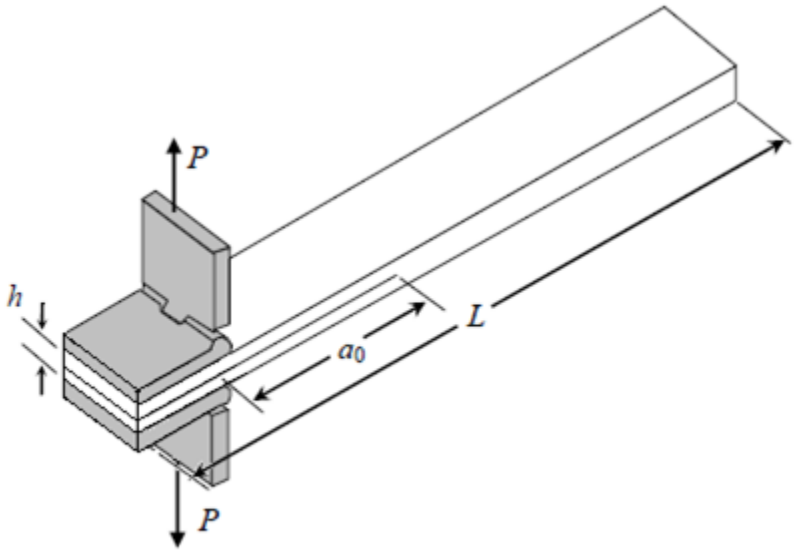


**Figure 15: Schematic of DCB specimen**

The sample dimensions of the DCB specimen used are enlisted in Table 3.

**Table 3: Sample dimensions for DCB testing**

| Dimensions | Values (inches) |
|---|---|
| **Length (L)** | 8 |
| **Width (b)** | 1 |
| **Depth (h)** | 0.16 |
| **Initial crack ($a_0$)** | 2 |

Testing was carried out on an instron 5587 machine, using tension clamps for holding the piano hinges. The crosshead speed used in the process (strain rate) was 1 mm/s. Load was applied using the load-cell of the machine and delamination length **'a'** was measured from the graduated edge of the specimen. The initial delamination length **'$a_0$'** was noted for further calculations. Instron interface software records the load deflection data and are tabulated in a '.raw' file. Readings for

the increments of delamination growth were noted down along with the corresponding load. Figure 16 shows the test setup and the final loaded sample.

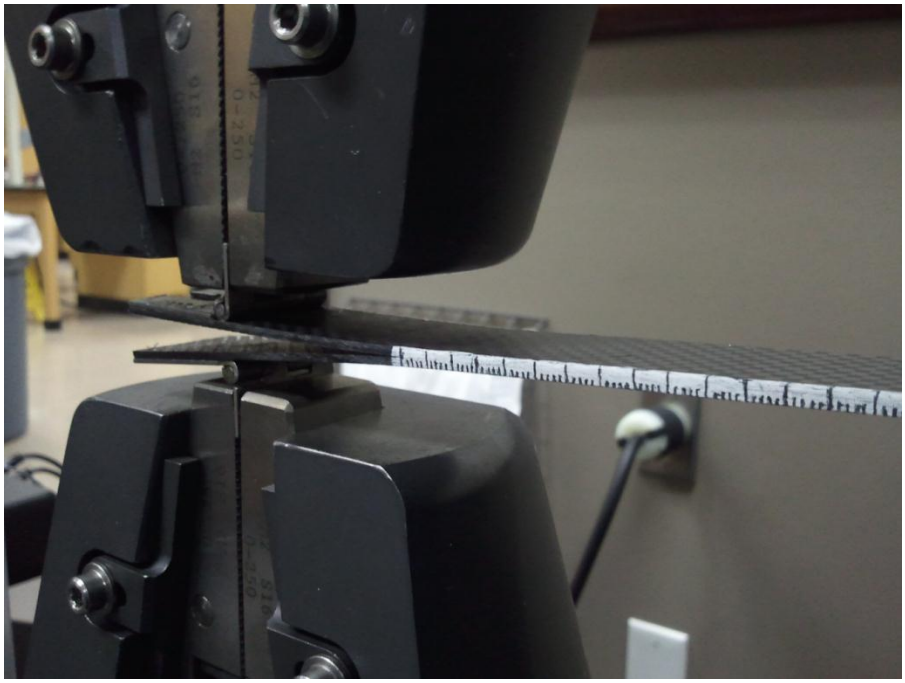

**Figure 16: Double Cantilever Testing**

The fracture toughness of the samples was calculated using a Modified Beam Theory Method. The beam theory expression for the strain energy release rate of a perfectly built-in double cantilever beam is given as follows.

$$G_I = \frac{3P\delta}{2b(a + |\Delta|)} \quad (2)$$

Where:

$P$ = load,

$\delta$ = load point displacement

$b$ = specimen width

$a$ = delamination length

$\Delta$ = correction factor

**Δ** is introduced in the original expression as a correction factor to account for the rotation of the delamination front as the beam is not exactly a built-in beam. The correction is accounted for by treating the DCB as having a slightly longer delamination ($a + |\Delta|$), where **Δ** is the x-intercept of a least squares plot of the cube root of compliance as a function of crack length. Figure 17 shows a root square plot for the calculation of error in the testing procedure.

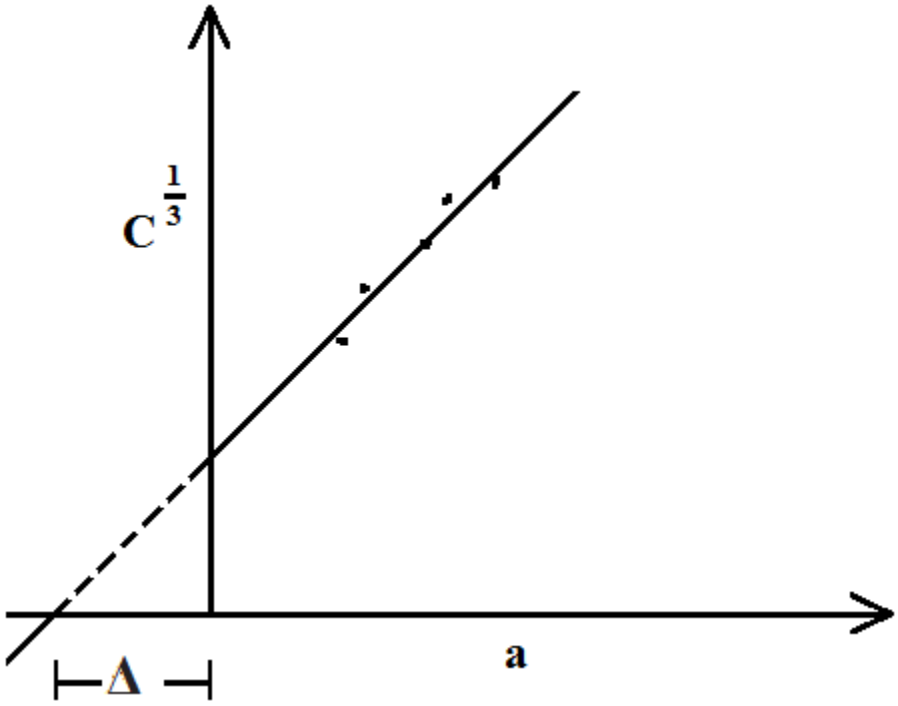


**Figure 17: Correction factor determination**

### 4.6 Fractography

The fracture surfaces of the delaminated samples from double cantilever beam test were studied for understanding the mechanism of fracture using a Hitachi S-4800 Scanning electron microscope (SEM).

### 4.7 Flexure testing

The flexural properties of the samples were measured by three point bending tests on the instron machine. Samples were prepared on the same lines as discussed earlier except for the point that the graphene oxide dispersed in PVP is painted on each of the 16 layers in the samples. The

specimen were cut from the composite laminates according to the ASTM standard, D 790 for testing flexural properties of reinforced plastics[83]. Figure 18 shows a specimen being tested on instron.

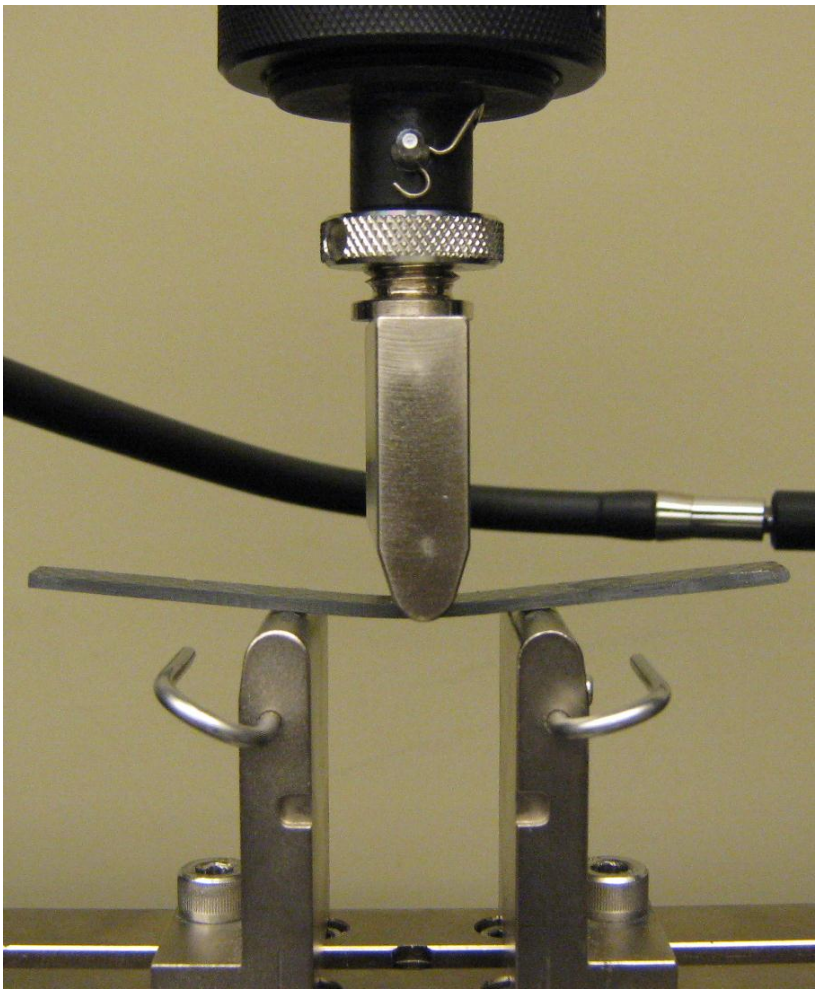

**Figure 18: Flexure testing on the laminate**

The sample dimensions of the flexural testing are enlisted in Table 4.

**Table 4: Sample dimensions for flexural testing**

| Dimensions | Values (inch) |
|---|---|
| Support span (L) | 2 |
| Width (b) | 1/2 |
| Depth (d) | 1/8 |

Testing was carried out on an instron machine 5528, using 3- point bending clamps with a crosshead speed of 0.275mm/min. Load was applied using the load-cell of the machine and the instron interface software records the load, deflection values. The flexural stress in the specimen was evaluated using classical beam theory assuming the beam to be elastic. A homogeneous elastic simply supported beam loaded at the midpoint has the maximum stress at the midsection and at the outermost fiber [84]. The equation relating the load applied and the flexural stress is given as

$$\sigma_f = \frac{3PL}{2bd^2} \quad \textbf{(3)}$$

Where:

$\sigma_f$ = flexural stress

$P$ = load at a given point on the load-deflection curve

$L$ = support span

$b$ = width of beam tested

$d$ = depth of beam tested

In the load displacement curves obtained, a toe region is observed, which is not the property of the material is. It shows an increased displacement with no applied load (or very low applied

load). This region may be attributed to alignment of the specimen in the loading process. In order to obtain correct measurements of the modulus and strength, the toe region is compensated and the calculations are carried out. Figure 19 shows a typical load-deflection curve with a toe region AC.

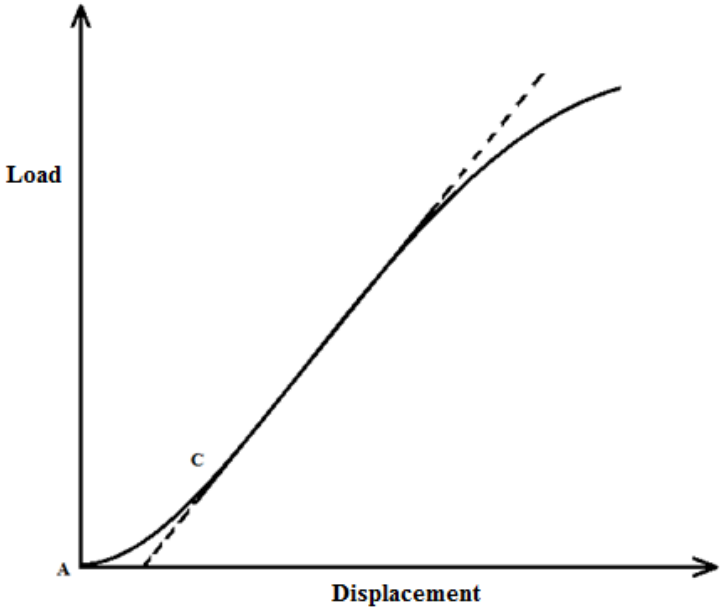


**Figure 19: Toe compensation**

# CHAPTER V

# RESULTS AND DISCUSSION

## 5.1 Graphene characterization

X-ray diffraction patterns collected in reflection, using a Bruker D8 Discovery diffractometer on graphite and graphene oxide powders are plotted in the Figure 20.

It can be observed from the plot that there is a difference in the intensity of the peaks, confirming that the densities of the materials are different (graphene oxide is less dense). Also, the graphene oxide diffraction pattern occurs at lower angles compared to graphite. This is an evidence of increase in the distance between the plates. The distance between the plates is calculated using the Bragg's law and the values are notified on the peaks in the plots. Similar peak patterns were observed by Peter Ho and colleagues and in their patent on functionalized graphene oxide [85]. The diffraction pattern for the graphite nanoparticles show characteristic peaks at $26.41^{o}$ and the same for graphene oxide occur at $10.53^{o}$. The d-spacing between the plates is calculated using the Bragg's law and is notified on the plot.

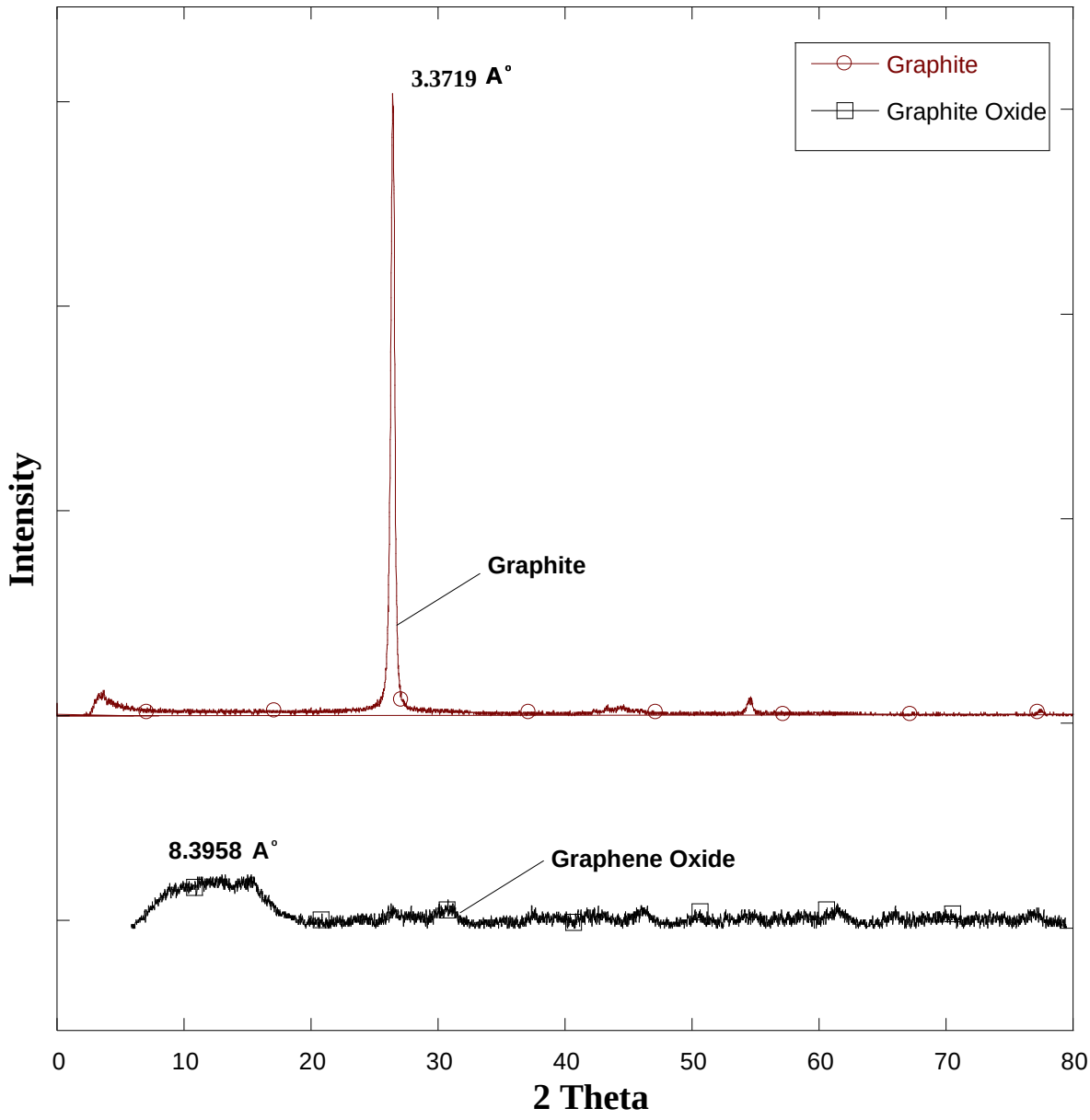


**Figure 20: X-Ray Diffraction analysis of graphene and graphene oxide**

### 5.2 Load vs. Deflection Curves (DCB)

The load and deflection recorded in the DCB testing are plotted and shown in the Figure 21 at different graphene oxide loadings. It can be inferred from the graph that the load required (energy absorbed) to propagate the crack in the specimen talks for the fracture toughness. Also, the

loading curve exhibits a saw tooth shaped profile, which is a characteristic of the stick-slip mode of crack propagation. Every sudden drop in the load can be attributed to crack propagation and the transition between the cracks to crack restriction. Similar load deflection pattern has been observed by Kathryn et al.in double cantilever testing of photopolymerizable (meth)acrylate polymer networks [86].

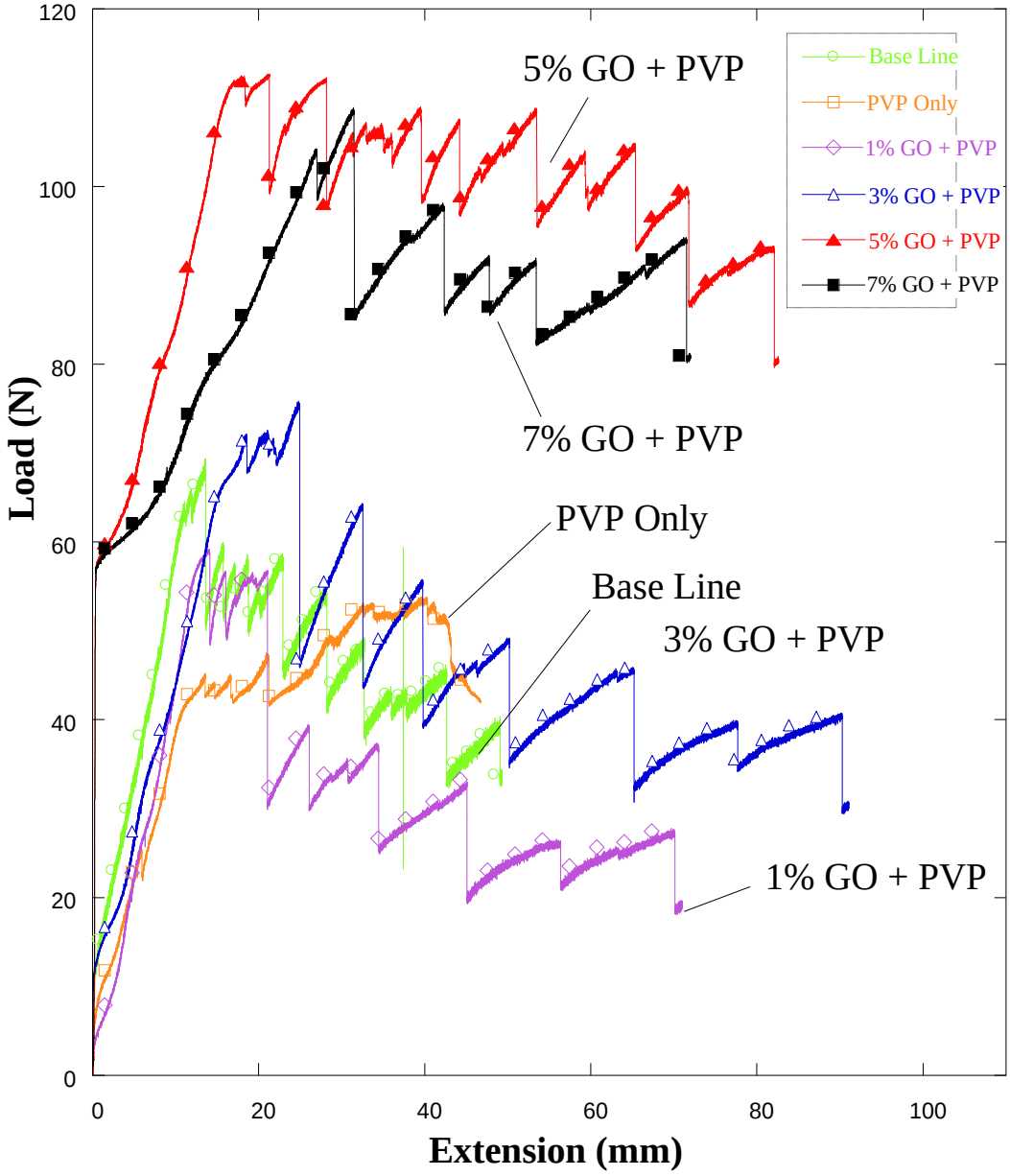


**Figure 21: Load vs. Extension plots - DCB**

Also, there is an increase in the modulus of the samples in 5 wt% and 7 wt% graphene oxide concentrations. This increase may be attributed to the increase in the crosslink density of the material due to the availability of functional groups. Kathryn et al. have reported similar behavior in photopolymerizable (meth) acrylate polymer networks [86].

### 5.2.1 Fracture Energy

From the double cantilever test results, critical strain energy release rate (Fracture toughness, $G_{IC}$) values were calculated using equation 2 and are tabulated in Table 5.

**Table 5: Propagation $G_{IC}$ at different filler content**

| Modification | $G_{IC}$ | Standard Deviation |
|---|---|---|
| **Base Line** | 818.17 | 34.34 |
| **PVP Only** | 1084.18 | 67.13 |
| **1% GO – PVP** | 708.62 | 35.18 |
| **3% GO – PVP** | 916.04 | 18.35 |
| **5% GO – PVP** | 1695.40 | 66.66 |
| **7% GO – PVP** | 1597.17 | 81.34 |

The $G_{IC}$ values are plotted in Figure 22. It can be seen from the bar chart that there is an improvement of approximately 30% in the fracture toughness with initial addition of PVP in the interface. Similar enhancement in the fracture toughness has been shown by Rutnakornpituk in "Thermoplastic Toughened Epoxy Networks and Their Toughening Mechanisms in Some Systems" with different thermoplastic materials in thermosetting resin systems [55].

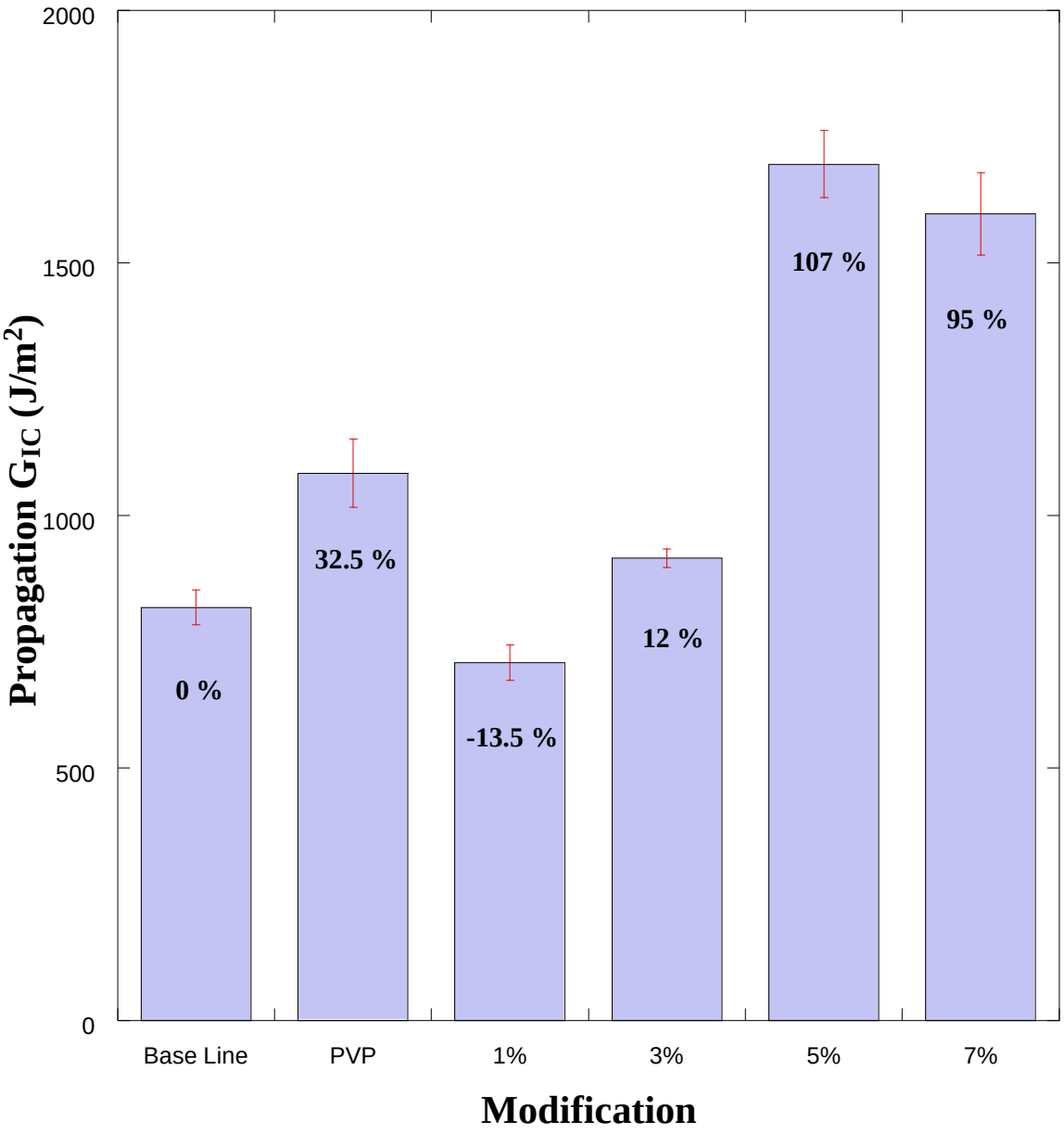


**Figure 22: Comparison of $G_{IC}$ at different filler contents**

Rutnakornpituk proposed that the mechanism of toughening might be that the thermoplastic additive could span two crack surfaces and apply surface tractions that counteract the stress required for the crack to advance. Also, the thermoplastic could phase separate and act as a crack deflector.

With an initial addition of graphene oxide (1% GO), there was a reduction in the fracture toughness. Since the graphene oxide is added to PVP solution prior to the application in the interface, some of the reactive groups within GO might be reacting with the amide and oxygen double bonds, making them unavailable to participate in the reaction with epoxide in the matrix resin.

When 5% GO – PVP was added to the interface, there was a drastic improvement in the $G_{IC}$. With further addition of GO after 5%, there is no significant change in the $G_{IC}$. Additionally, beyond 5% GO, agglomeration effects could become significant, similar to observations by Ke Wang et al, with clay additives in "Epoxy Nanocomposites with Highly Exfoliated Clay: Mechanical Properties and Fracture Mechanisms" [18].

### 5.2.2 Resistance curves

Resistance curves are the plots signifying variation in strain energy release with an increase in crack length. Figure 23 shows the resistance curves at different filler content. It can be seen that there is an improvement in the propagation fracture toughness of laminates containing 5 and 7 wt % of graphene oxide in the interface. Also, it can be inferred from the plot that the crack is unstable while propagating. This can be attributed to the modification of bonding between fiber and epoxy interface. Similar behavior is observed by  in [87].

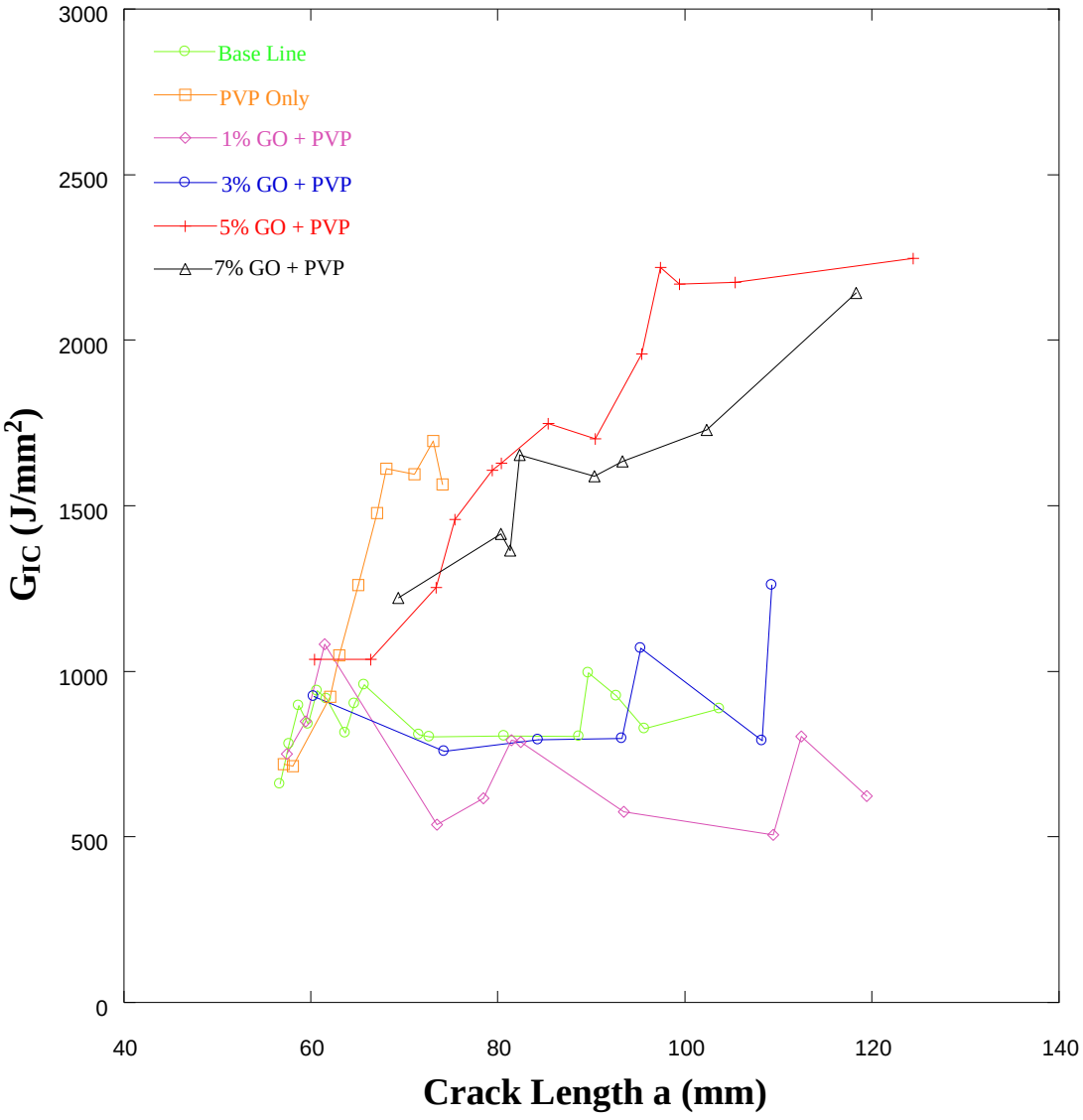


**Figure 23: R- Curves for DCB**

### 5.3 SEM, TEM Analysis and Fractography

SEM analysis on the un-exfoliated and exfoliated graphene oxide was carried out and the results are shown in the Figure 24. It can be seen from the SEM images that the plates are seen separated and distance between the plates has significantly improved.

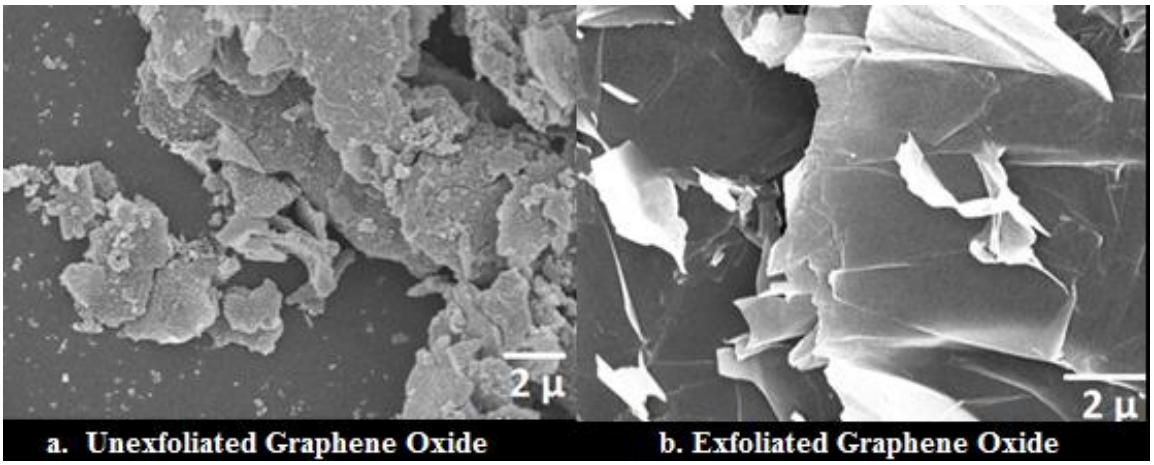


**Figure 24: (a.) Unexfoliated and (b.) Exfoliated Graphene Oxide**

TEM analysis on the PVP intercalated graphene oxide was carried out and the results are shown in Figure 25. Layered structure of graphene oxide can be seen from the TEM image and the separation between the layers can be understood.

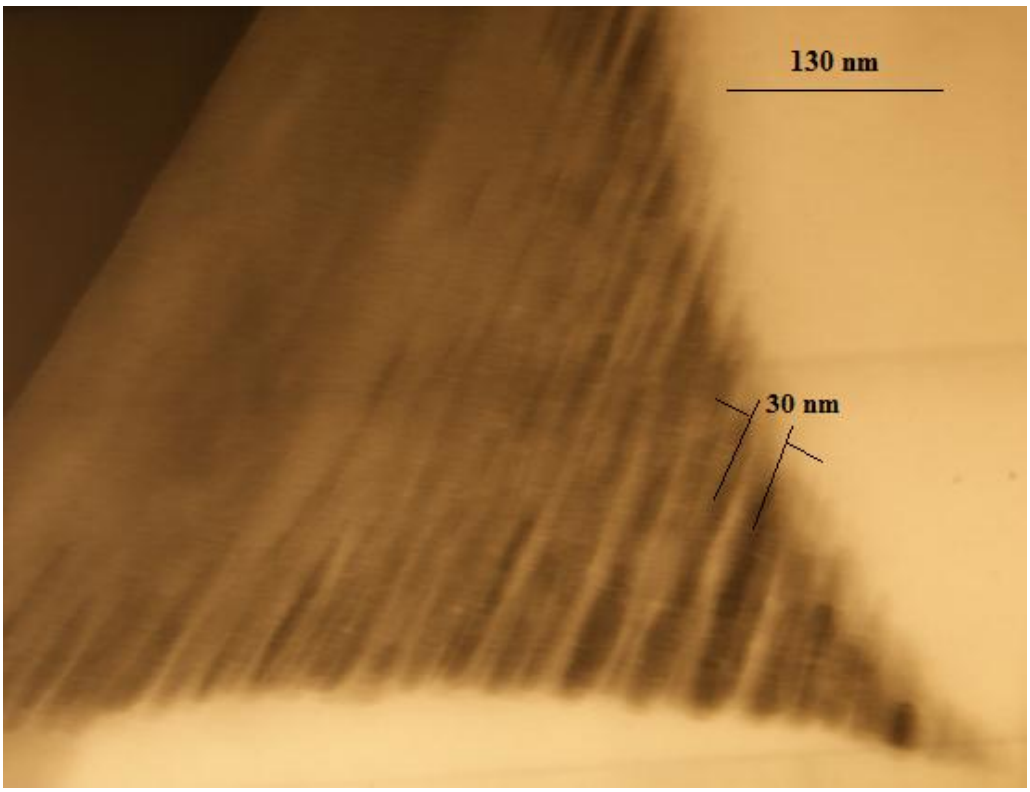


**Figure 25: TEM image of PVP - GO film**

Fracture surface analysis of the DCB samples revealed that intercalation is well achieved. Figure 26 shows an SEM image that shows the fracture surface of a specimen tested using DCB. It can be seen from the fracture surface that the resin system also contributes to the separation of the graphene oxide plates.

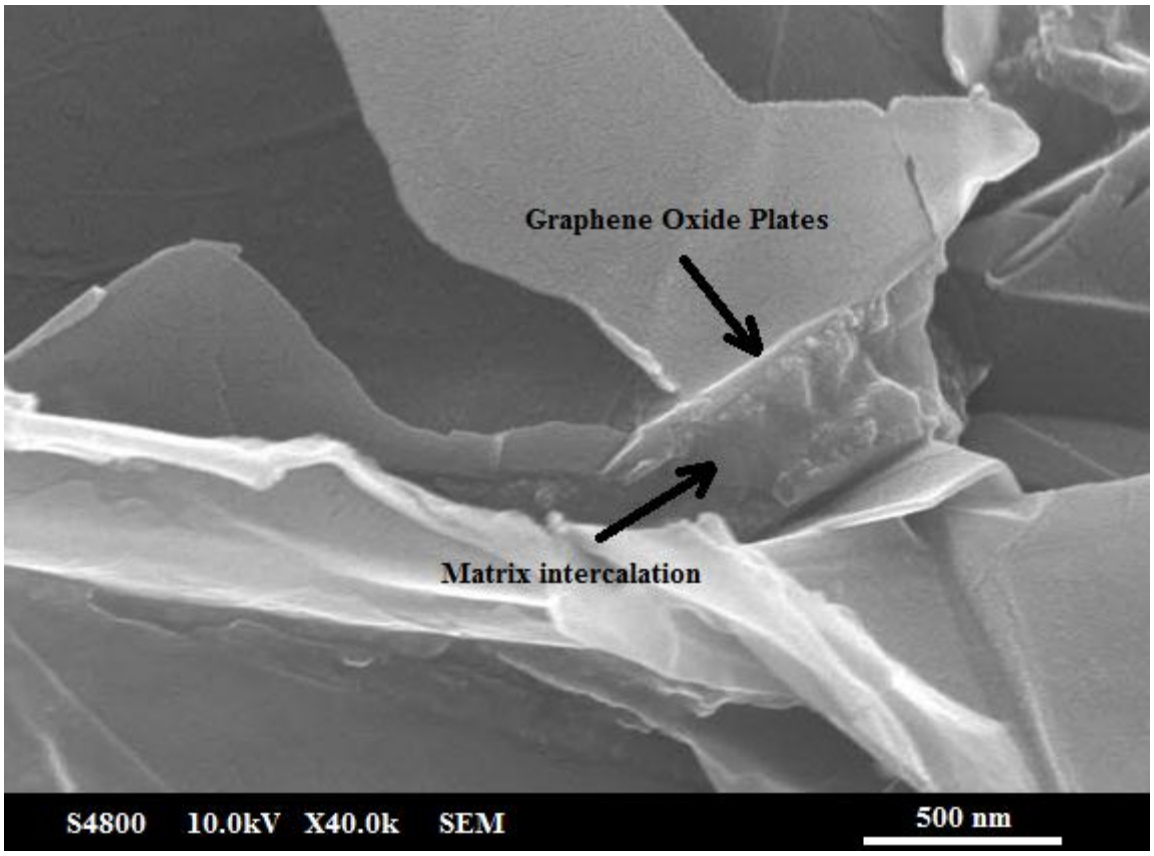


**Figure 26: Resin system intercalated between two graphene oxide layers**

The fracture surfaces of the specimen after DCB testing were studied usning a SEM and the fracture mechanisms are predicted. Figure 27 is an SEM image at X 5.00k magnification of the crack surfaces of plain composite and 5 wt% graphene oxide composite. It can be seen in the figure that the fracture surface of the neat epoxy is very smooth except for few river like markings near the tip of the crack. This type of fractograph is typical for brittle polymers, proving that the resistance to crack is very low [18]. On the other side, the fracture surface of graphene

oxide modified composite is rougher when compared to that of plain composite.

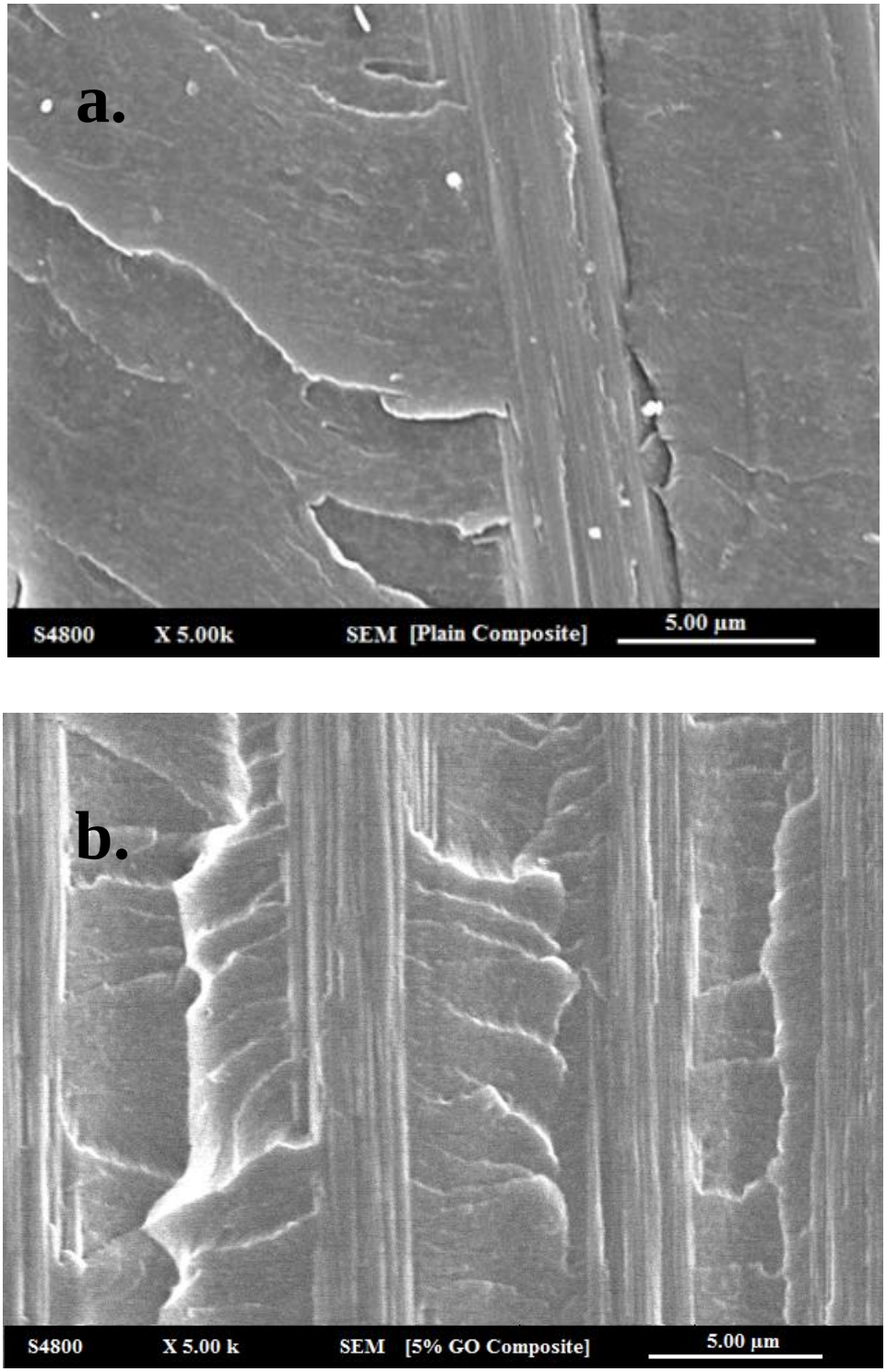


**Figure 27: Surface morphology of crack surface a. baseline Composite b. 5% GO- PVP**

### 5.3.1 Addition of PVP

As it is seen that there is an initial improvement in the fracture toughness with the addition of PVP, the fracture surfaces have been studied. The fractograph of mode I failure specimen is shown in Figure 28.

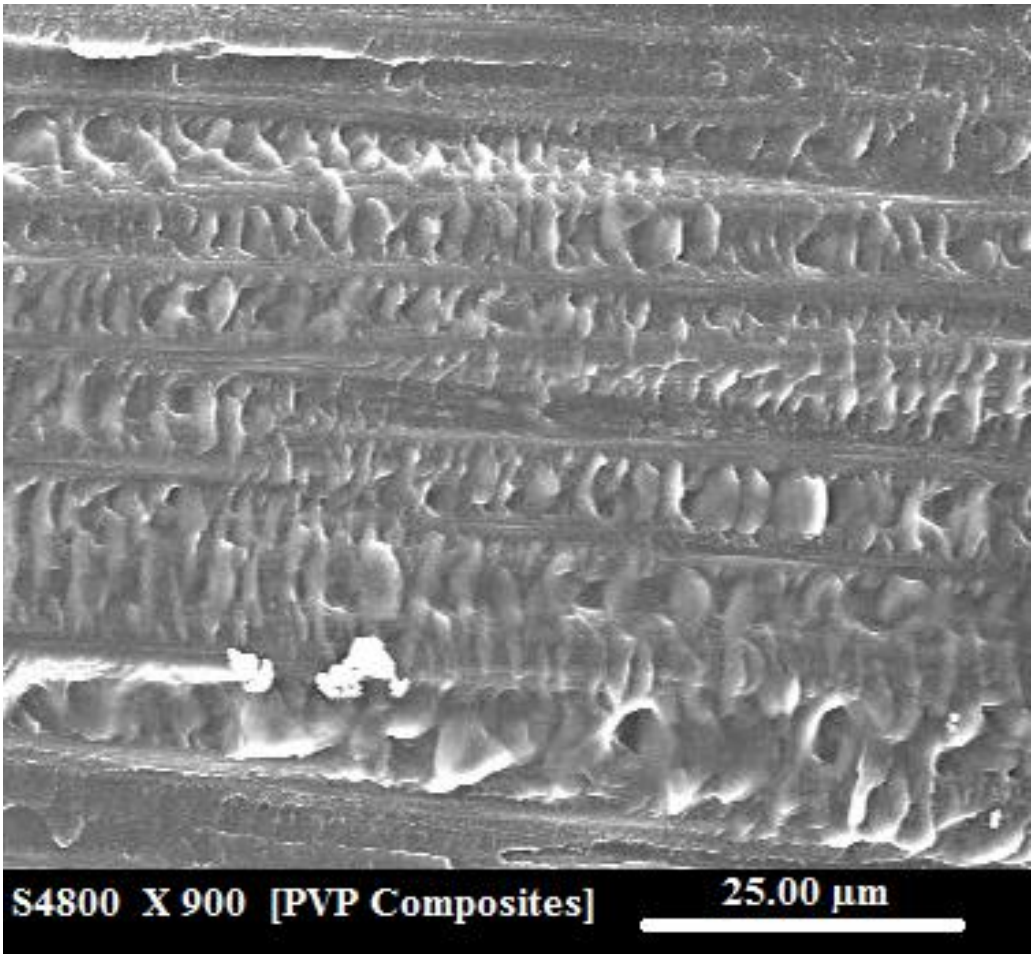


**Figure 28: Fracture surface of PVP composite**

It can be observed from the fracture surface that there is a lot of plastic flow involved in the process.

### 5.3.2 Reduction in $G_{IC}$ with 1-3 wt% of GO

From the fracture toughness values from the DCB results, it has been observed that there is a reduction in the $G_{IC}$ values with an initial addition of graphene oxide (1-3 wt % of GO) in the interface. Fractographic studies of mode I failed DCB specimen revealed that there is a uniform distribution of phase separated PVP- graphene oxide particles of large particle size. These particles might act as inclusions in the composites and result in lowering of fracture toughness. The formation of phase separations in a 3 wt% graphene oxide specimen is shown in Figure 29. These phases are clearly visible on the crack interface because the crack travelled through the phases. The possible reason behind formation of these agglomerates is unavailability of reactive groups in PVP – graphene oxide solution. This might result in formation of stable PVP – graphene oxide phase in the interface.

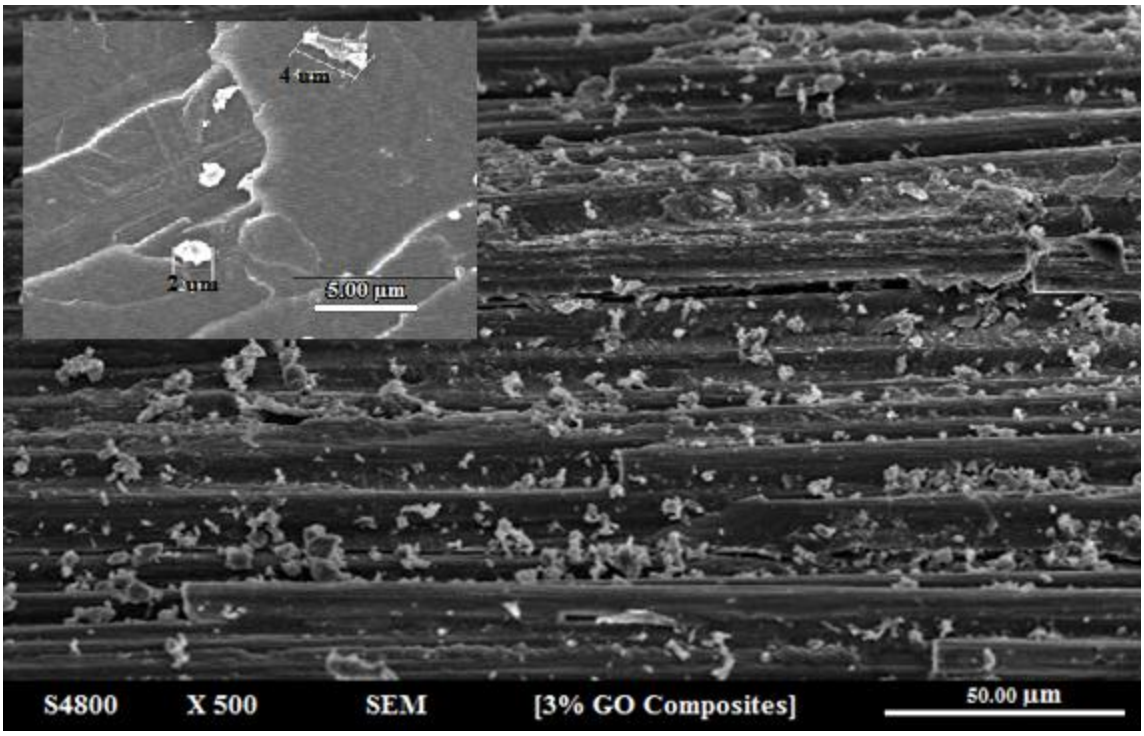


**Figure 29: PVP - phase separation**

However, crack deflection and other toughening phenomenon have also been observed in 3 wt% graphene oxide composites, despite phase separation. These occurrences can well explain the increase in the fracture toughness in the laminates from 1wt % to 3% GO addition (Figure 30).

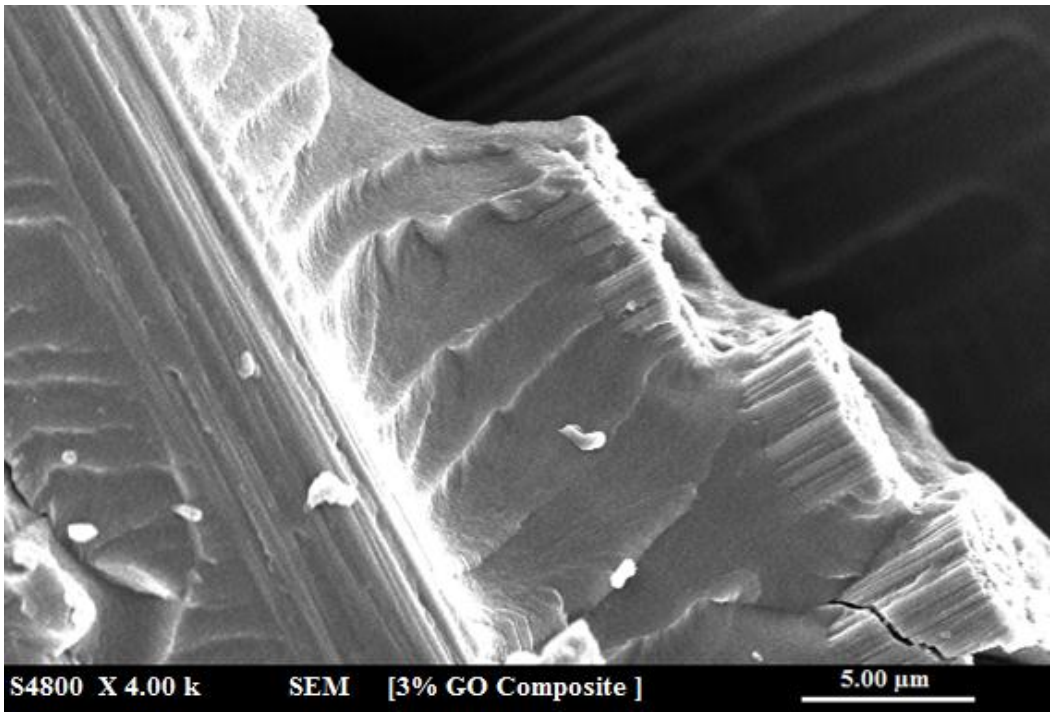


**Figure 30: Surface morphology of 3% GO composite**

### 5.3.3 $G_{IC}$ between 1-7 wt % of GO

SEM fractographs have been taken for the DCB specimen for understanding the mechanism of toughening by graphene oxide toughening.

The SEM image shown in Figure 31 describes the crack deflection occurring in the composites at 5 % graphene oxide concentration. It can be observed from the image that the fracture surface is very rough and filled with scale-like steps. This is an indication of the presence of graphene oxide layers in the interface, forcing the crack to take a much tortuous propagate along a very tortuous path.

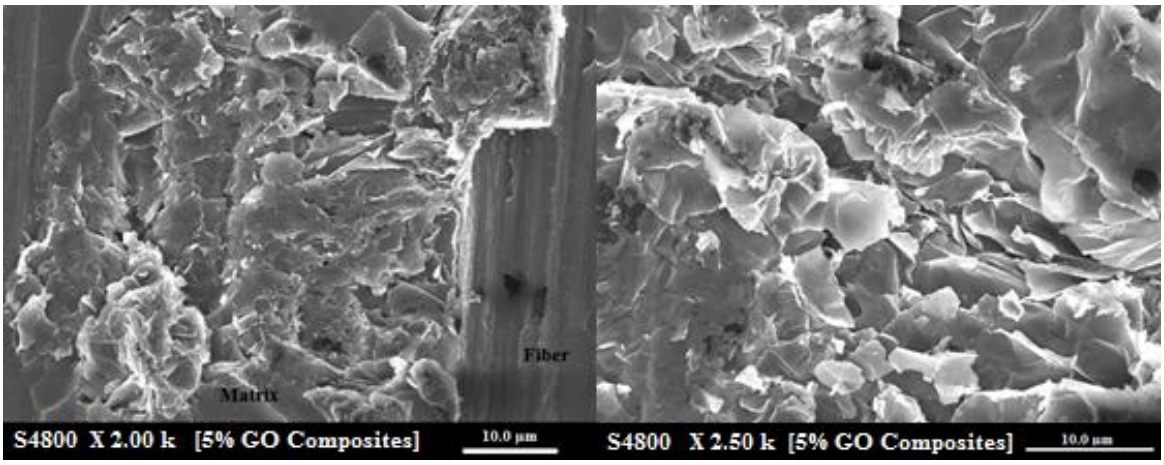


**Figure 31: Crack deflection in 5% GO composites.**

Crack arresting and jumping patterns are observed on the fracture surface of the laminates, which relate to the saw-tooth profile on the load vs. displacement curve. Figure 32: Crack Jumping and arresting patterns on composites compares crack jumping phenomenon in 1 and 5 wt % graphene oxide composites. It can be seen from the SEM image that the number of jumps becomes larger with the increase of GO concentration, indicating high crack deflection. Hussain et al. observed similar crack jumping behavior in titanium dioxide filled epoxies [88].

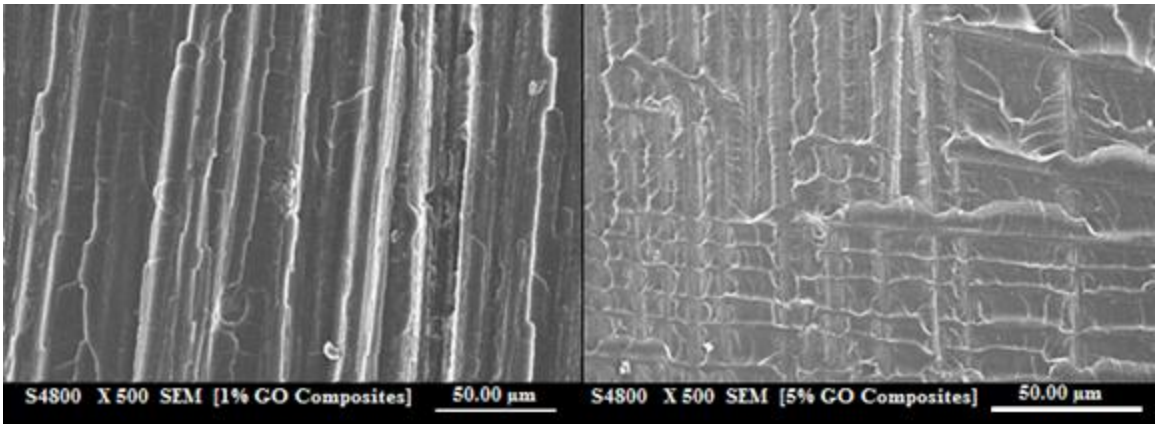


**Figure 32: Crack Jumping and arresting patterns on composites**

Advantage of crack jumping and arresting is that it releases large amounts of energy, leading to plastic deformation of the matrix phase. Plastic deformation blunts the crack and helps in further energy absorption at the crack tip.

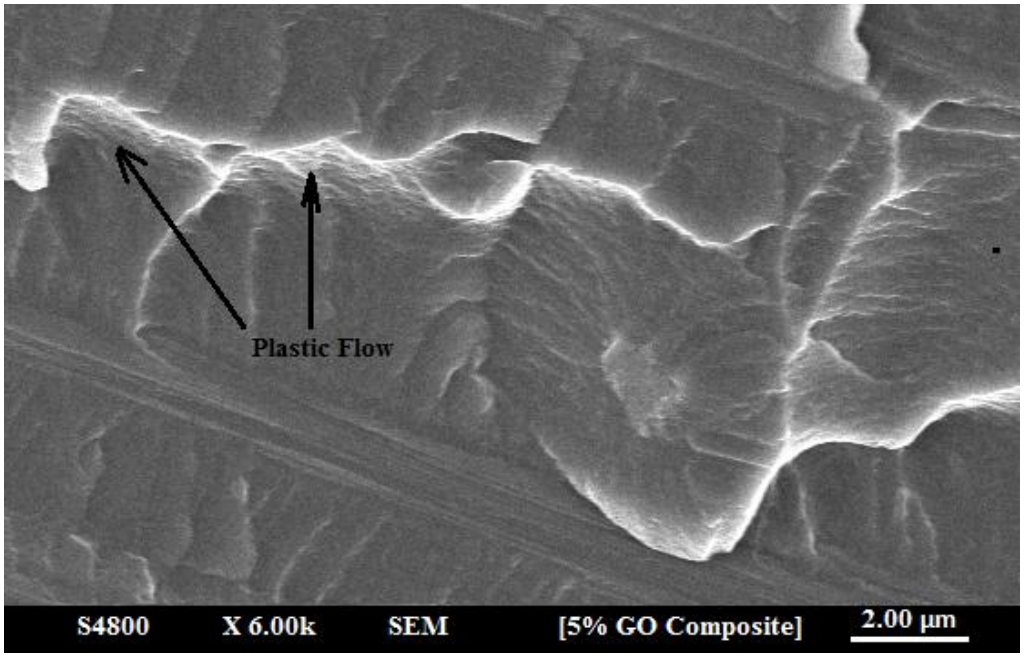


**Figure 33: Plastic Deformation**

Figure 33: Plastic Deformation shows plastic flow at the crack-tip in a 5 wt% graphene composite laminate. Similar pattern has been observed by Han and his colleagues when they incorporated fumed silica nanoparticles [89]. Crack pinning is another observed phenomenon in graphene oxide filled composites. Figure 34 shows crack pinning mechanism in 5 wt% graphene oxide composites.

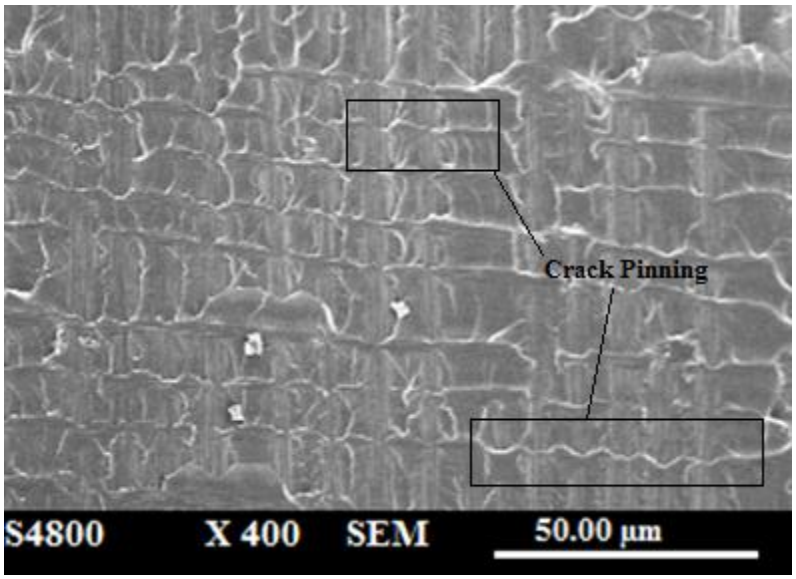


**Figure 34: Crack pinning**

### 5.3.4 Microcracking

Another mechanism of fracture observed is by the mechanical cleaving of the layered graphene oxide. Though graphene is termed as a single crystal, any configuration that has 10 layers or below is generally termed as 2D [51, 90]. In this case, the intercalated and exfoliated graphene oxide will still be a group of few plates and those plates trap microcracks in the composites, which can grow with application of load. Figure 35 shows the concept of crack initiation in layered nanocomposites.

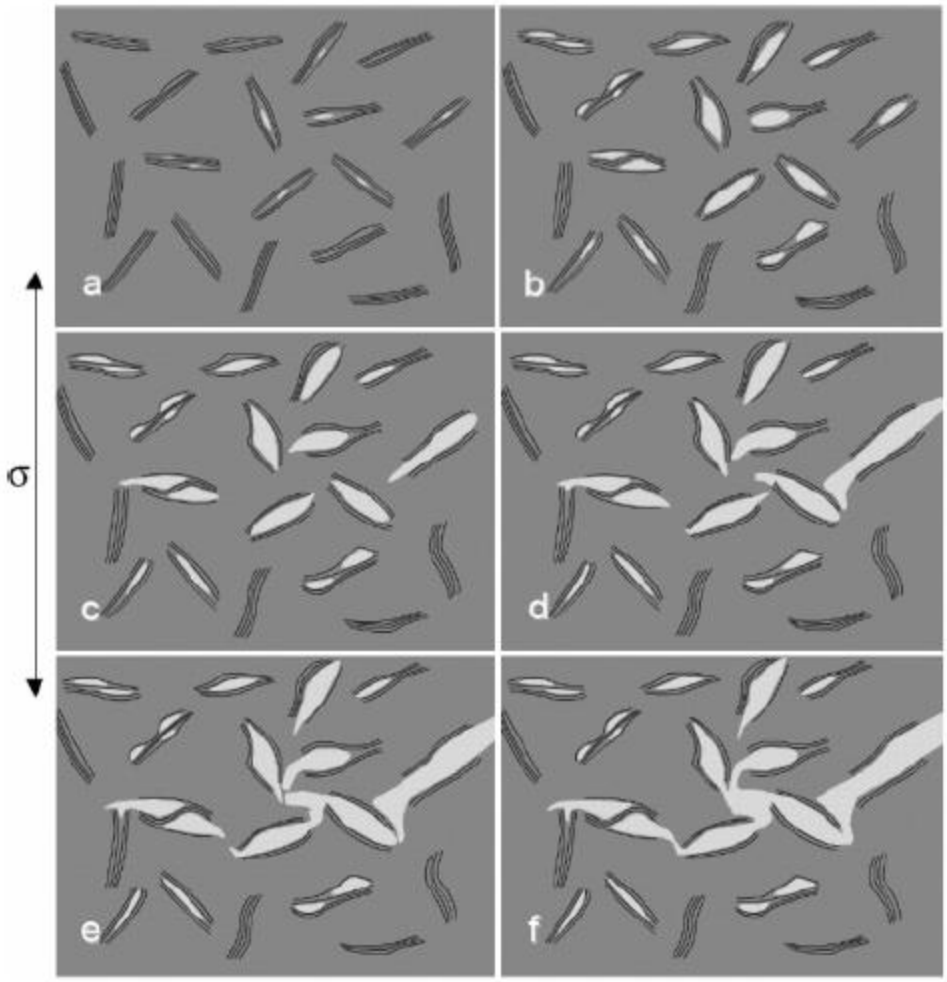


**Figure 35: Crack initiation and propagation in composites with layered fillers [18]**

Figure 36 shows the microcracking phenomenon observed in 7 wt % graphene oxide composites. It can be seen from the figure that there is a good bonding between the plates and the matrix. The smooth plate surface is an evidence for separation of the plates by the load applied. Also, a clear edge on the surface of the plate supports the fact that the plate surface has been hidden from the matrix and has been exposed after mechanical cleavage occurred.

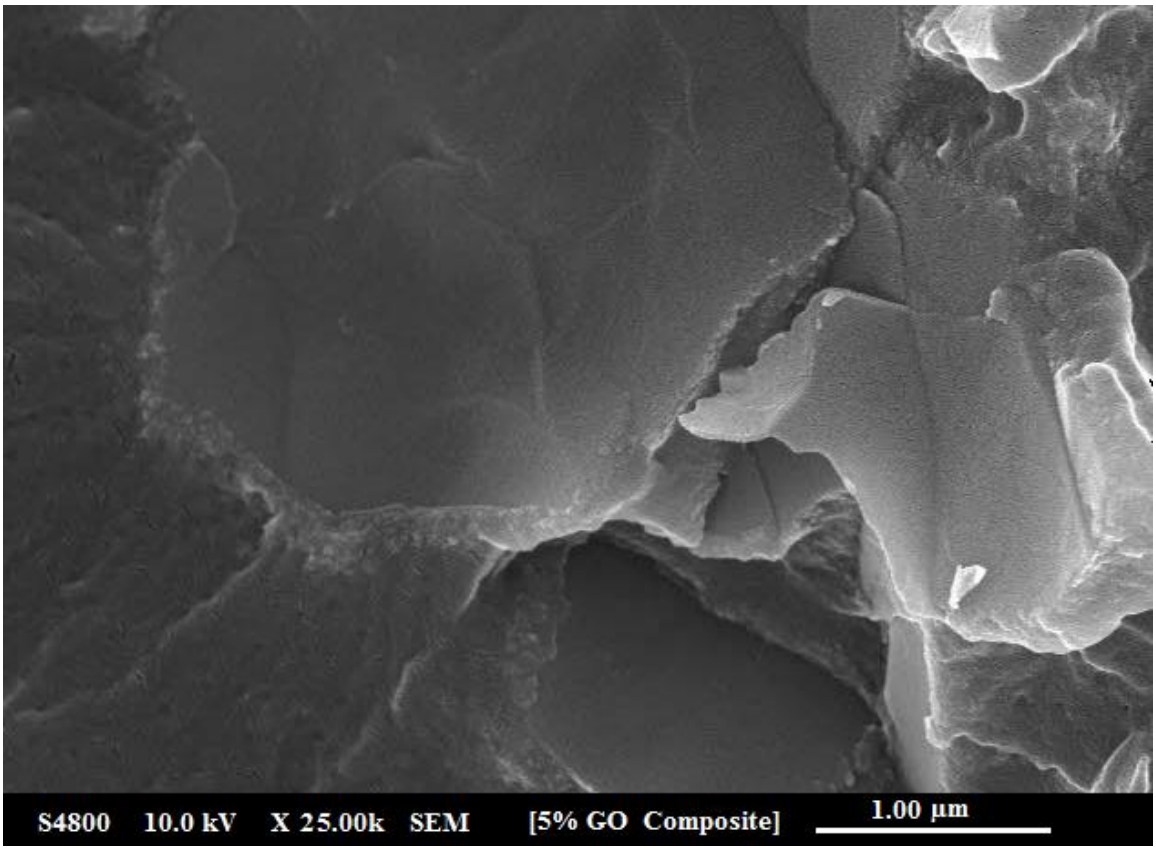


Figure 36: Micro cracking phenomenon

## 5.4 Flexural Testing

Stress vs. strain data is evaluated from the load deflection curves in flexure following the astm standard. The data is plotted in the Figure 37 and it can be observed that there is a drop in the flexural strength of the composite laminates. Also, the toe region in the stress vs. strain plots can be observed. Similar toe like regions have been observed by Lu et al. on interleaved carbon/epoxy composite laminates [91].

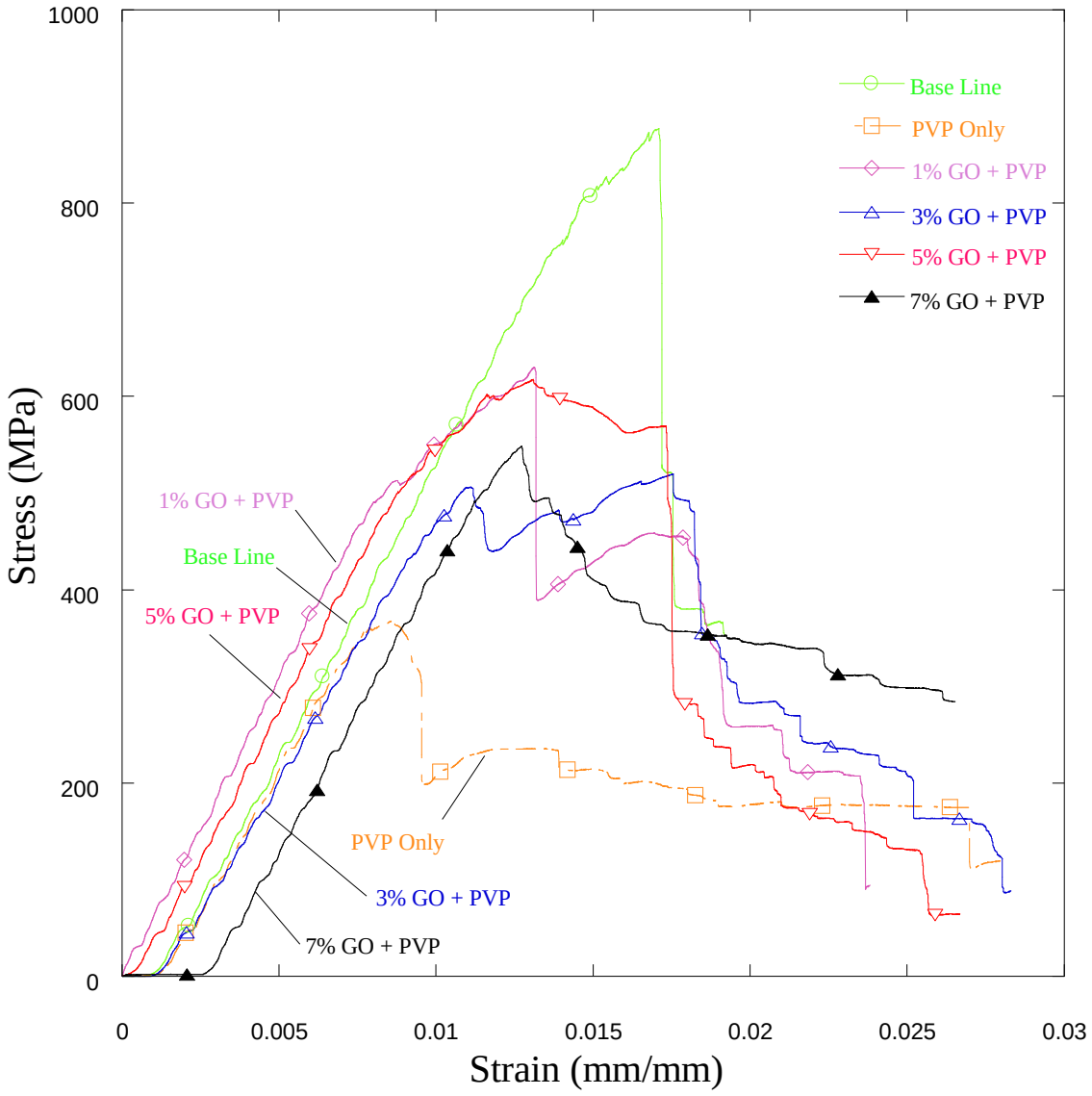


**Figure 37: Stress - Strain curves in flexure**

Toe compensation is corrected and stress vs. strain plots are re-plotted in Figure 38 till elastic region to obtain flexural modulus.

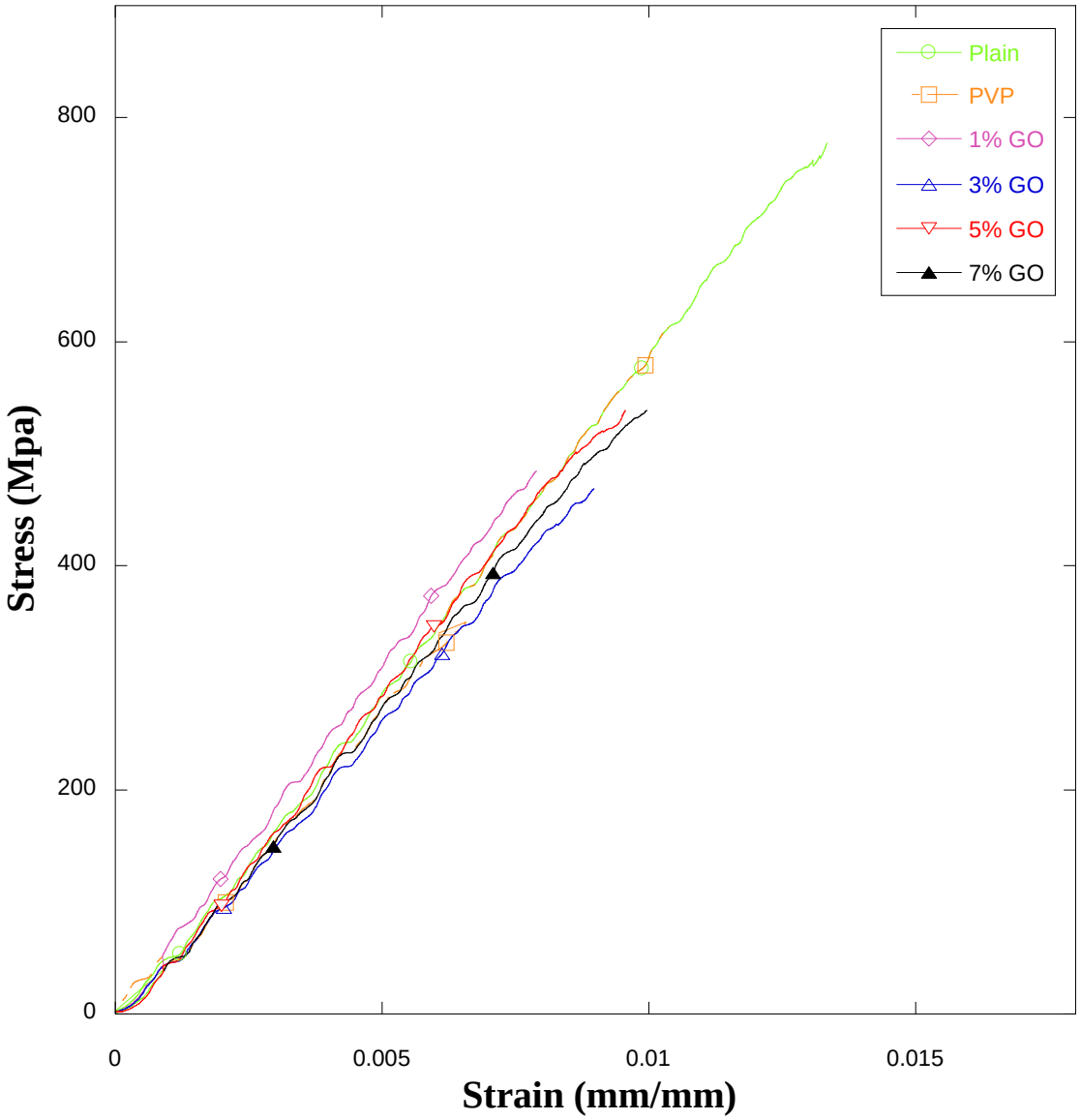


**Figure 38: Modulus calculation**

The results on the flexural modulus are are plotted in Figure 39: Flexural Modulus and tabulated in Table 6. It can be observed from the plot that there is no significant effect of different treatments on the flexural modulus. Similar behavior is observed by Yuan Li et al. with the use of vapor grown carbon fiber nanofillers at the mid-plane of CFRP laminates [34].

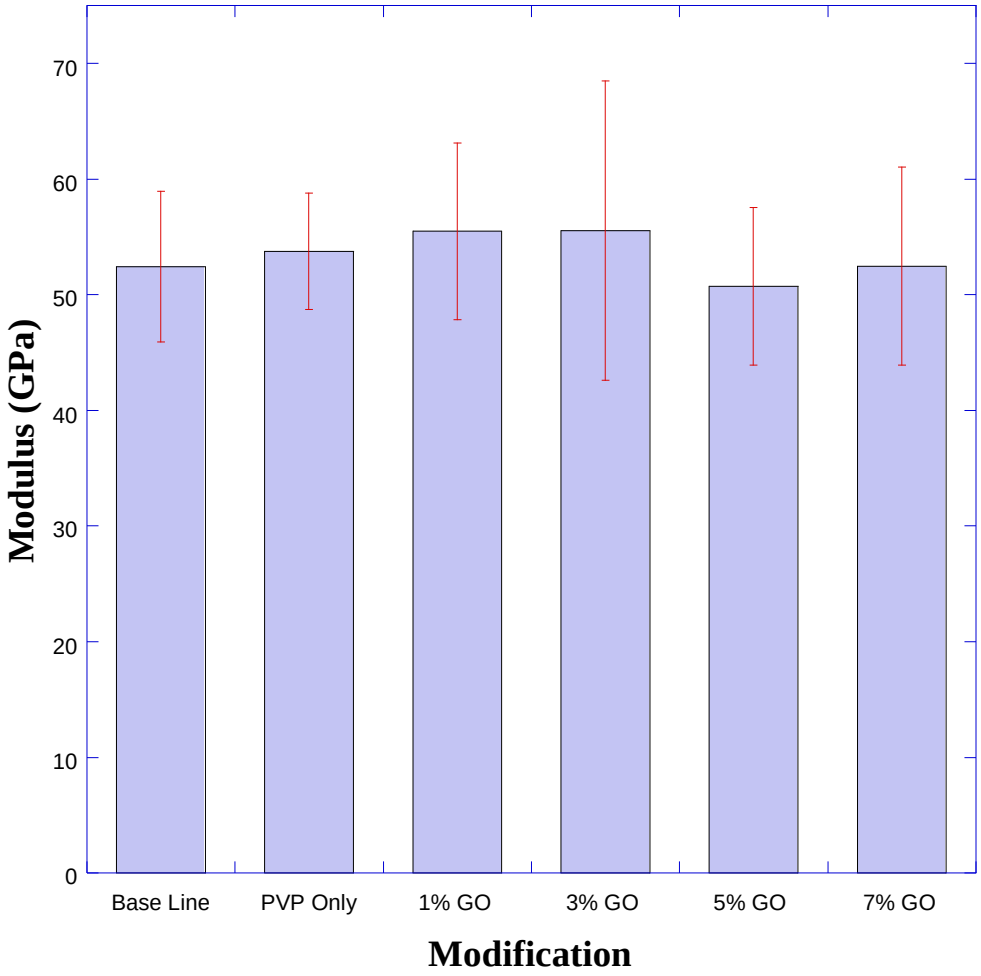


Figure 39: Flexural Modulus

Table 6: Flexural Modulus

| Modification | Modulus (GPa) | Standard Deviation |
|---|---|---|
| Plain Composite | 52.42 | 6.51 |
| PVP-Composite | 53.75 | 5.02 |
| 1% GO Composite | 55.48 | 7.63 |
| 3% GO Composite | 55.53 | 12.96 |
| 5% GO Composite | 50.73 | 6.8 |
| 7% GO Composite | 52.47 | 8.54 |

### 5.5 Toughness – Flexural modulus tradeoff

In most of the modification techniques, with every toughness improvement, there is an associated reduction in other properties [55]. That is, there is always a tradeoff between toughness and other properties. In our case, flexural properties are expected to reduce due to nonhomogeneous material properties in the through thickness direction [91]. It is observed in our case that there is no significant change in the flexural modulus with improvement in the toughness. Figure 40 shows a plot that shows tradeoff between toughness and flexural modulus.

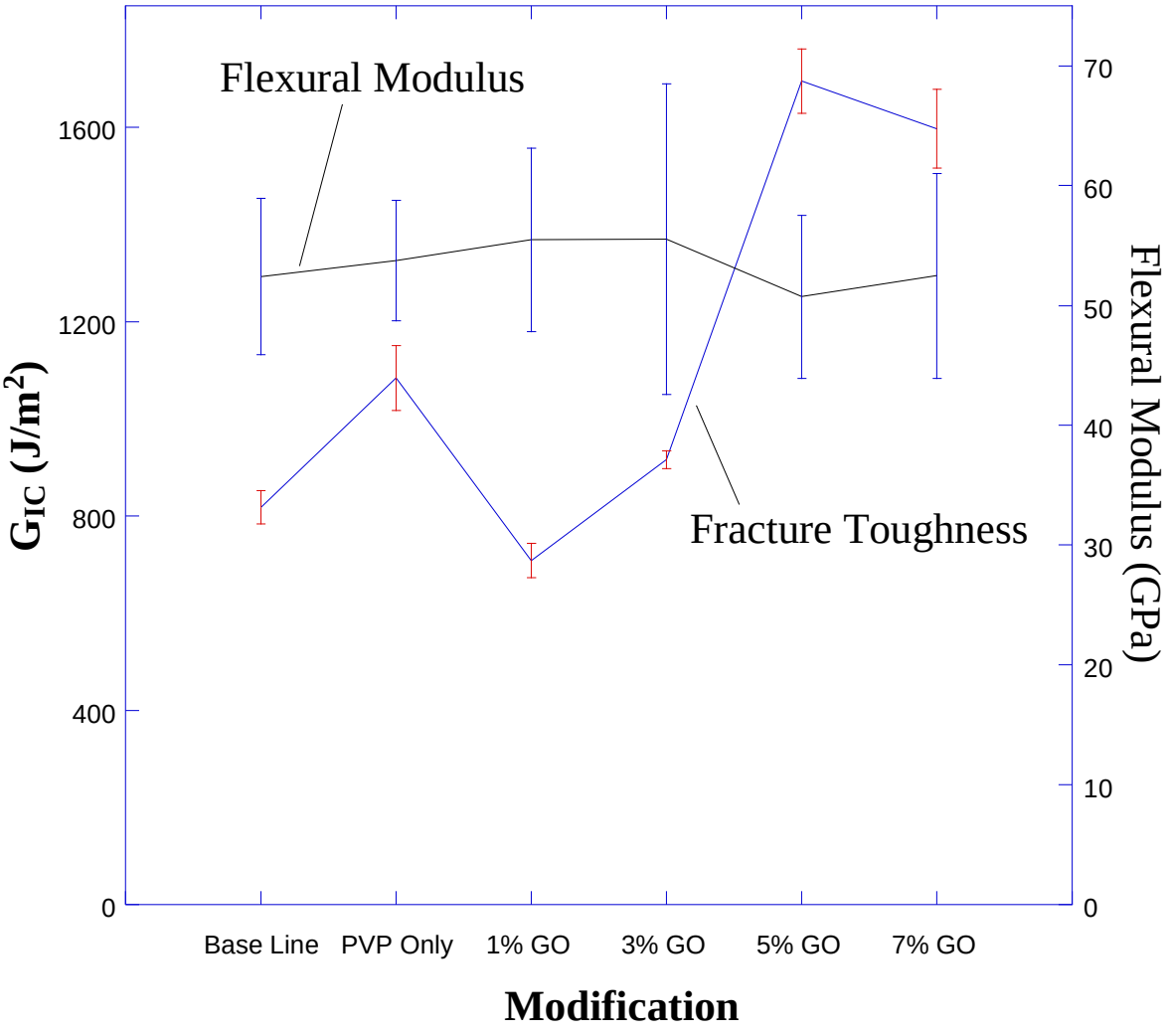


**Figure 40: Toughness - Flexural modulus tradeoff**

Figure 41 describes the correlation between fracture toughness and flexural modulus. It can be seen from the plot that the trend of fracture toughness improvement has a high slope. In other words, improvement in fracture toughness can be obtained without a reduction in flexural modulus (not significant change).

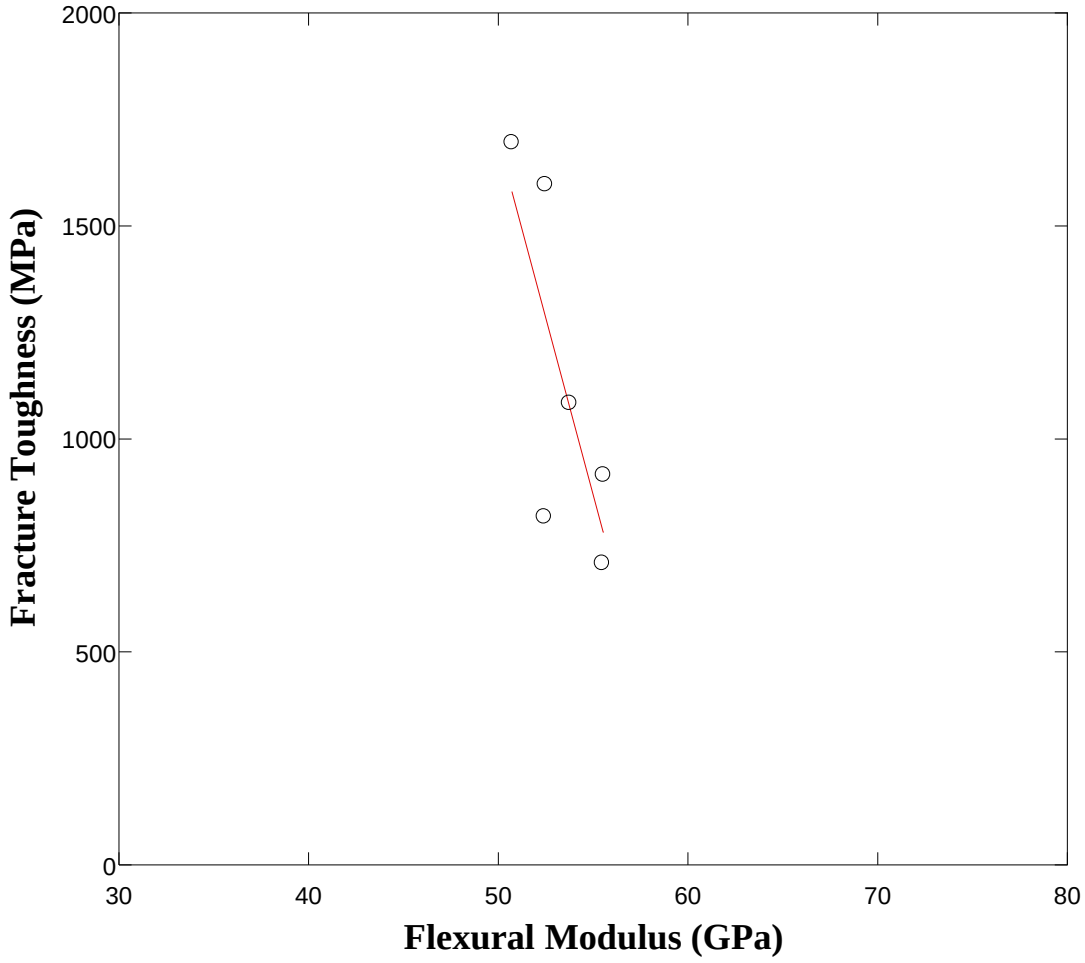


**Figure 41: Fracture Toughness vs. Flexural Modulus**

# CHAPTER VI

## CONCLUSION AND SCOPE

A smart selective toughening method that uses graphene oxide as secondary filler has been developed in the current study. Carbon fiber reinforced epoxy resins have been modified with PVP dispersed graphene oxide in the interface region and fracture toughness and flexural strength have been evaluated. A 100% improvement in the fracture toughness with as little as 5 weight percent of graphene oxide in the interface has been achieved. Unlike typical toughening methods, this enhancement has been achieved without sacrificing flexural modulus properties of the composites.

In an industrial applicability standpoint, realization of lab scale research with a minimal initial investment and easy technology transfer is critical. The present work is an effort to achieve enhancement in the mechanical properties of materials in a way that can easily be adapted to the industry with least possible effort and cost. The process can easily be automated and at low material costs.

Table 7 is a comparison of filler content used in various literature, corresponding increase in the fracture toughness and rough estimate of the filler prices (cost per unit improvement of $G_{IC}$) the data in Table 7 is plotted in Figure 42. It can be observed that the suggested method in the current study economically enhances the fracture toughness compared to other fillers.

**Table 7: Comparison of various literature and their rough price listing**

| Filler Type | Filler Content | $G_{IC}$ | Price ($/1% improvement) |
|---|---|---|---|
| **GO** | 0.02 | 100 | 0.03 |
| **Alumina [66]** | 0.2 | 51 | 0.04 |
| **Alumina [66]** | 0.2 | 74 | 0.03 |
| **CNTs [92]** | 5 | 97 | 0.46 |
| **Clay [13]** | 7 | 100 | 0.01 |
| **CNTs [34]** | 12.7 | 26 | 2.5 |

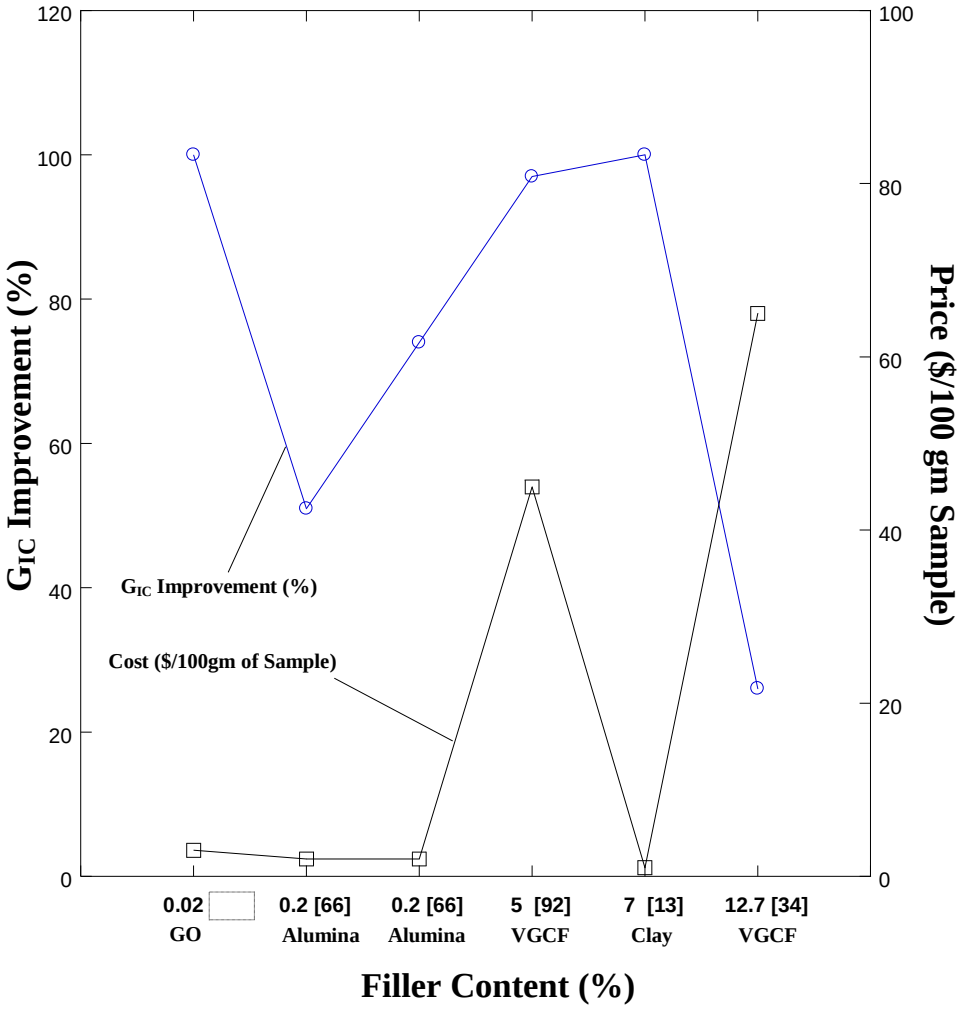


**Figure 42: Comparison of $G_{IC}$, Cost and Filler Content in literature**

It is known that graphene oxide is hydrophilic and thus may have some effect on the hygroscopic properties of composites. Thus a detailed study on the hygroscopic effects on the GO modified composites would give an idea of the applicability of these composites.

Further suggestions for improvement of the study will be to develop a micromechanical model that can predict the toughness properties of graphene oxide filled composites. A three phase model similar to the one used by Zhang et al. can be used to predict the mechanical properties of the composites [93].

REFERENCES


[1] Aveston, Cooper and Kelly , "Single and multiple fracture," in *The properties of fibre composites*, National Physics Laboratory, IPC Science and technology Press Ltd., 1971, pp. 15-26.

[2] (September 29, 2010, 01/15/2011 ). *Epoxy Resins: A Global Strategic Business Report*. Available: http://www.StrategyR.com/

[3] D. Ratna, *Handbook of thermoset resins*: Smithers Rapra Technology, 2009

[4] T. Scherzer, "Characterization of diol modified epoxy resins by near- and mid-infrared spectroscopy," *Journal of Applied Polymer Science,* vol. 51, pp. 491-502, 1994.

[5] J. McElvain, M. Keshavarz, H. Wang, F. Wudl, A. J. Heeger, "Fullerene-based polymer grid triodes," *Journal of Applied Physics,* vol. 81, pp. 6468-6472, 1997.

[6] C. Li and Tsu-Wei Chou, "A structural mechanics approach for the analysis of carbon nanotubes," *International Journal of Solids and Structures,* vol. 40, pp. 2487-2499, 2003.

[7] S. Tkachev, E. Buslaeva, S. Gubin, "Graphene: A novel carbon nanomaterial," *Inorganic Materials,* vol. 47, pp. 1-10, 2011.

[8] J. A. VanderVennet, Duenas, Y. Terrisa Dzenis, Chad T. Peterson, Charles E. Bakis, D. Carter, J. K. Roberts, "Fracture toughness characterization of nanoreinforced carbon-fiber composite materials for damage mitigation," San Diego, California, USA, 2011, pp. 797823-10.

[9] W. F. Hosford, *Mechanical behavior of materials* Newyork: Cambridge university press, 2005.

[10] K. Trakasl and K. Mark, *The relationship between critical strain energy release rate and fracture mode in multidirectional carbon-fiber/epoxy laminates,* vol. 6. Ann Arbor: American Society for Testing Materials, 1997.

[11] S. Chatterjee, F. A. Nuesch, B. T. T. Chu, "Comparing carbon nanotubes and graphene nanoplatelets as reinforcements in polyamide 12 composites," *Nanotechnology* vol. 22 pp. 1-8, 25 May 2011.

[12] T. Yokozeki, Y. Iwahori, M. Ishibashi, T. Yanagisawa, K. Imai,M. Arai, T. Takahashi, K. Enomoto, "Fracture toughness improvement of CFRP laminates by dispersion of cup-stacked carbon nanotubes," *Composites Science and Technology,* vol. 69, pp. 2268-2273, 2009.

[13] N. A. Siddiqui, R. S. C. Woo, Jang-Kyo Kim, C. C. K. Leung, A. Munir, "Mode I interlaminar fracture behavior and mechanical properties of CFRPs with nanoclay-filled epoxy matrix," *Composites Part A: Applied Science and Manufacturing,* vol. 38, pp. 449-460, 2007.

[14] H. T. Oyama, J. J. Lesko, J. P. Wightman, "Interdiffusion at the interface between poly(vinylpyrrolidone) and epoxy," *Journal of Polymer Science Part B: Polymer Physics,* vol. 35, pp. 331-346, 1997.

[15] K. T. Faber and A. G. Evans, "Crack deflection processes--I. Theory," *Acta Metallurgica,* vol. 31, pp. 565-576, 1983.

[16] K. T. Faber and A. G. Evans, "Crack deflection processes--II. Experiment," *Acta Metallurgica,* vol. 31, pp. 577-584, 1983.

[17] M. A. Rafiee, J. Rafiee, I. Srivastava, Z. Wang, H. Song, Zhong-Zhen Yu, N. Koratkar, "Fracture and Fatigue in Graphene Nanocomposites," *Small,* vol. 6, pp. 179-183, 2010.

[18] K. Wang, L. Chen, J. Wu, M. L. Toh, C. He, A. F. Yee, "Epoxy Nanocomposites with Highly Exfoliated Clay: Mechanical Properties and Fracture Mechanisms," *Macromolecules,* vol. 38, pp. 788-800, 2005.

[19] T. Ramanathan, A. A. Abdala, S. Stankovich, D. A. Dikin, A. M. Herrera R. D. Piner, D. H. Adamson, H. C. Schniepp, X. Chen, R. S. Ruoff, S. T. Nguyen, I. A. Aksay, R. K. Prud'Homme, L. C. Brinson, "Functionalized graphene sheets for polymer nanocomposites," *Nat Nano,* vol. 3, pp. 327-331, 2008.

[20] B. S. P. C. Bockrath, Derrick, "Application of exfoliation techniques to the preparation of MoS2 liquefaction catalysts," in *Coal Science and Technology*. vol. Volume 24, J. A. Pajares and J. M. D. Tascón, Eds., ed: Elsevier, 1995, pp. 1343-1346.

[21] G. Swaminathan and K. Shivakumar, "Thermomechanical and Fracture Properties of Exfoliated Nanoclay Nanocomposites," *Journal of Reinforced Plastics and Composites,* February 7, 2011 2011.

[22] N. V. Medhekar,*A.* Ramasubramaniam, R. S. Ruoff, V. B. Shenoy, "Hydrogen Bond Networks in Graphene Oxide Composite Paper: Structure and Mechanical Properties," *ACS Nano,* vol. 4, pp. 2300-2306, 2010.

[23] S. Yoon and I. In, "Role of poly(N-vinyl-2-pyrrolidone) as stabilizer for dispersion of graphene via hydrophobic interaction," *Journal of Materials Science,* vol. 46, pp. 1316-1321, 2011.

[24] F. Hubertus and Q. Anisul, "Polyvinylpyrrolidone (PVP) – One of the Most Widely Used Excipients in Pharmaceuticals: An Overview," *Drug Delivery Technology,* vol. 8, June 2008.

[25] M. Munz,*J.* Chung, G. Kalinka, "Mapping Epoxy Interphases," in *Adhesion*, ed: Wiley-VCH Verlag GmbH & Co. KGaA, 2006, pp. 103-123.

[26] M. Szczerba, *J.* Srodon, M. Skiba, A. Derkowski, "One-dimensional structure of exfoliated polymer-layered silicate nanocomposites: A polyvinylpyrrolidone (PVP) case study," *Applied Clay Science*, vol. 47, pp. 235-241, 2010.

[27] C. M. Koo, H. T. Ham, M. H. Choi,S. O. Kim, I. J. Chung, "Characteristics of polyvinylpyrrolidone-layered silicate nanocomposites prepared by attrition ball milling," *Polymer,* vol. 44, pp. 681-689, 2003.

[28] M. Alexandre and P. Dubois, "Polymer-layered silicate nanocomposites: preparation, properties and uses of a new class of materials," *Materials Science and Engineering: R: Reports,* vol. 28, pp. 1-63, 2000.

[29] L. Vaisman, H. D. Wagner, G. Marom, "The role of surfactants in dispersion of carbon nanotubes," *Advances in Colloid and Interface Science,* vol. 128-130, pp. 37-46, 2006.

[30] Z. Liang, *R.* Lao, J. Wang, Y. Liu, L. Wang, Q. Huang, S. Song, G. Li, C. Fan, "Solubilization of Single-walled Carbon Nanotubes with Single- stranded DNA Generated from Asymmetric PCR," *International Journal of Molecular Sciences,* vol. 8, pp. 705-713, 2007.

[31] D. J. Unger, *Analytical Fracture Mechanics*. San Diego: Academic Press, 1995.

[32] E. J. Winn and I. W. Chen, "Crack Deflection in Composites with Very Thin Interlayers," *Journal of the American Ceramic Society,* vol. 83, pp. 3222-3224, 2000.

[33] W. X. Wang, Y. Takao, T. Matsubara, H. S. Kim, "Improvement of the interlaminar fracture toughness of composite laminates by whisker reinforced interlamination," *Composites Science and Technology,* vol. 62, pp. 767-774, 2002.

[34] Y. Li, N. Hori, M. Arai, N. Hu, Y. Liu, H. Fukunaga, "Improvement of interlaminar mechanical properties of CFRP laminates using VGCF," *Composites Part A: Applied Science and Manufacturing,* vol. 40, pp. 2004-2012, 2009.

[35] J.-C. Huang, "Carbon black filled conducting polymers and polymer blends," *Advances in Polymer Technology,* vol. 21, pp. 299-313, 2002.

[36] M. Moniruzzaman,*J.* Chattopadhyay, W. E. Billups,K. I. Winey, "Tuning the Mechanical Properties of SWNT/Nylon 6,10 Composites with Flexible Spacers at the Interface," *Nano Letters,* vol. 7, pp. 1178-1185, 2007.

[37] D. R. Dreyer, S. Park, C. W. Bielawski,R. S. Ruoff, "The chemistry of graphene oxide," *Chemical Society Reviews,* vol. 39, pp. 228-240, 2010.

[38] W. S. Hummers and R. E. Offeman, "Preparation of Graphitic Oxide," *Journal of the American Chemical Society,* vol. 80, pp. 1339-1339, 1958.

[39] J.-L. Tsai and J.-F. Tu, "Characterizing mechanical properties of graphite using molecular dynamics simulation," *Materials & Design,* vol. 31, pp. 194-199, 2010.

[40] J. W. McClure, "Band Structure of Graphite and de Haas-van Alphen Effect," *Physical Review,* vol. 108, p. 612, 1957.

[41] C. Lee, X. Wei, J. W. Kysar,J. Hone, "Measurement of the Elastic Properties and Intrinsic Strength of Monolayer Graphene," *Science,* vol. 321, pp. 385-388, July 18, 2008 2008.

[42] J. S. Bunch, "Mechanical and electrical properties of graphene sheets," Doctor of Philosophy Dissertation, Graduate School of Cornell University, 2008.

[43] H. C. Schniepp, Je-Luen Li, M. J. McAllister, H. Sai, M. Herrera-Alonso, D. H. Adamson,R. K. Prud'homme, R. Car, D. A. Saville, I. A. Aksay, "Functionalized Single Graphene Sheets Derived from Splitting Graphite Oxide," *The Journal of Physical Chemistry B,* vol. 110, pp. 8535-8539, 2006.

[44] D. Zhan, L. Sun,Z. H. Ni, L. Liu, X. F. Fan, Y. Wang, T. Yu, Y. M. Lam, W. Huang, Z. X. Shen, "FeCl3-Based Few-Layer Graphene Intercalation Compounds: Single Linear Dispersion Electronic Band Structure and Strong Charge Transfer Doping," *Advanced Functional Materials,* vol. 20, pp. 3504-3509, 2010.

[45] B. Jayasena and S. Subbiah, "A novel mechanical cleavage method for synthesizing few-layer graphenes," *Nanoscale Research Letters,* vol. 6, p. 95, 2011.

[46] S. Burcu, O. Firuze D. Fatma Y. Yuda, "Enhanced exfoliation technique for the separation of graphene nanosheets," presented at the 6th Chemical Engineering

Conference for collaborative research in Eastern Mediterranean countries: EMCC-6, Belek, Antalya, Turkey, 2010.

[47] Xiao-ping Wang, An-min, Huang, De-min Jia, Yan-mei Li, "From exfoliation to intercalation--changes in morphology of HNBR/organoclay nanocomposites," *European Polymer Journal*, vol. 44, pp. 2784-2789, 2008.

[48] Z. Zhang and M. M. Lerner, "Preparation, Characterization, and Exfoliation of Graphite Perfluorooctanesulfonate," *Chemistry of Materials*, vol. 8, pp. 257-263, 1996.

[49] D. D. L. Chung, "Exfoliation of graphite," *Journal of Materials Science*, vol. 22, pp. 4190-4198, 1987.

[50] H. Xia and M. Song, "Intercalation and exfoliation behaviour of clay layers in branched polyol and polyurethane/clay nanocomposites," *Polymer International*, vol. 55, pp. 229-235, 2006.

[51] A. K. Geim and K. S. Novoselov, "The rise of graphene," *Nat Mater*, vol. 6, pp. 183-191, 2007.

[52] N. D. Mermin, "Crystalline Order in Two Dimensions," *Physical Review*, vol. 176, p. 250, 1968.

[53] A. S. Argon and R. E. Cohen, "Toughenability of polymers," *Polymer*, vol. 44, pp. 6013-6032, 2003.

[54] J. A. De Souza, S. Goutianos, M. Skovgaard, B. F. Sørensen, "Fracture resistance curves and toughening mechanisms in polymer based dental composites," *Journal of the Mechanical Behavior of Biomedical Materials*, vol. 4, pp. 558-571, 2011.

[55] M. Rutnakornpituk, "Thermoplastic Toughened Epoxy Networks and Their Toughening Mechanisms in Some Systems," *Naresuan University Journal*, vol. 13, pp. 73-83, 12 April 2005.

[56] D. J. Hourston, S. Lane,H. X. Zhang, "Toughened thermoplastics: 2. Impact properties and fracture mechanisms of rubber modified poly(butylene terephthalates)," *Polymer,* vol. 32, pp. 2215-2220, 1991.

[57] P. Weiss, "Toughened plastics, C. B. Bucknall, Applied Science Publishers, Ltd., London, 1977, 359pp," *Journal of Polymer Science: Polymer Letters Edition,* vol. 16, pp. 376-376, 1978.

[58] Y. H. Huang, D. L. Kinloch Anthony, J. Riew, C. Keith, "Mechanisms of Toughening Thermoset Resins," in *Toughened Plastics I*. vol. 233, ed: American Chemical Society, 1993, pp. 1-35.

[59] A. C. Balazs, T. Emrick, T. P. Russell, "Nanoparticle Polymer Composites: Where Two Small Worlds Meet," *Science,* vol. 314, pp. 1107-1110, November 17, 2006 2006.

[60] M. Moniruzzaman, *et al.*, "Increased flexural modulus and strength in SWNT/epoxy composites by a new fabrication method," *Polymer,* vol. 47, pp. 293-298, 2006.

[61] De Morais, A. B. de Moura, M. F. Marques, A. T. de Castro, "Mode-I interlaminar fracture of carbon/epoxy cross-ply composites," *Composites Science and Technology,* vol. 62, pp. 679-686, 2002.

[62] M. Rafiee, F. Yavari, J. Rafiee, N. Koratkar, "Fullerene–epoxy nanocomposites-enhanced mechanical properties at low nanofiller loading," *Journal of Nanoparticle Research,* vol. 13, pp. 733-737, 2011.

[63] D. Mao, "Improving mechanical properties of nanocomposites using carbon nanotubes," in *Society for the Advancement of Material and Process Engineering*, 2009, pp. 1-8.

[64] F. Zhao and Y. Huang, "Improved interfacial properties of carbon fiber/epoxy composites through grafting polyhedral oligomeric silsesquioxane on carbon fiber surface," *Materials Letters,* vol. 64, pp. 2742-2744, 2010.

[65] Y. Huang, Y. Qin, Y. Zhou, H. Niu, Zhong-Zhen Yu, Jin-Yong Dong, "Polypropylene/Graphene Oxide Nanocomposites Prepared by In Situ Ziegler−Natta Polymerization," *Chemistry of Materials*, vol. 22, pp. 4096-4102, 2010.

[66] A. D. Kelkar, R. Mohan, R. Bolick,S. Shendokar, "Effect of nanoparticles and nanofibers on Mode I fracture toughness of fiber glass reinforced polymeric matrix composites," *Materials Science and Engineering: B*, vol. 168, pp. 85-89, 2010.

[67] S. N. Yadav, V. Kumar, S. K. Verma, "Fracture toughness behaviour of carbon fibre epoxy composite with Kevlar reinforced interleave," *Materials Science and Engineering: B*, vol. 132, pp. 108-112, 2006.

[68] L. Liu, A. H. Barber, S. Nuriel, H. D. Wagner, "Mechanical Properties of Functionalized Single-Walled Carbon-Nanotube/Poly(vinyl alcohol) Nanocomposites," *Advanced Functional Materials*, vol. 15, pp. 975-980, 2005.

[69] H. Dodiuk, S. Kenig, I. Blinsky, A. Dotan, A. Buchman, "Nanotailoring of epoxy adhesives by polyhedral-oligomeric-sil-sesquioxanes (POSS)," *International Journal of Adhesion and Adhesives*, vol. 25, pp. 211-218, 2005.

[70] T. T. Baby and S. Ramaprabhu, "Investigation of thermal and electrical conductivity of graphene based nanofluids," *Journal of Applied Physics*, vol. 108, pp. 124308-6, 2010.

[71] C. Min and D. Yu, "Simultaneously improved toughness and dielectric properties of epoxy/graphite nanosheet composites," *Polymer Engineering & Science*, vol. 50, pp. 1734-1742, 2010.

[72] I. Zaman, T. T. Phan, Hsu-Chiang Kuan, Q. Meng, Ly Truc Bao La, L. Luong, O. Youssf,J. Ma, "Epoxy/graphene platelets nanocomposites with two levels of interface strength," *Polymer*, vol. 52, pp. 1603-1611, 2011.

[73] X. Yang, Y. Tu, L. Li, S. Shang, Xiao-ming Tao, "Well-Dispersed Chitosan/Graphene Oxide Nanocomposites," *ACS Applied Materials & Interfaces*, vol. 2, pp. 1707-1713, 2010.

[74] H. Fan, L. Wang, K. Zhao, N. Li, Z. Shi, Z. Ge, Z. Jin, "Fabrication, Mechanical Properties, and Biocompatibility of Graphene-Reinforced Chitosan Composites," *Biomacromolecules,* vol. 11, pp. 2345-2351, 2010.

[75] B. J. Cardwell and A. F. Yee, "Toughening of epoxies through thermoplastic crack bridging," *Journal of Materials Science,* vol. 33, pp. 5473-5484, 1998.

[76] S. A. Meguid, "Mechanics and mechanisms of toughening of advanced ceramics," *Journal of Materials Processing Technology,* vol. 56, pp. 978-989, 1996.

[77] V. R. Mastelaro and E. D. Zanotto, "Residual stresses in a soda-lime-silica glass-ceramic," *Journal of Non-Crystalline Solids,* vol. 194, pp. 297-304, 1996.

[78] B. Wetzel, P. Rosso, F. Haupert, K. Friedrich, "Epoxy nanocomposites - fracture and toughening mechanisms," *Engineering Fracture Mechanics,* vol. 73, pp. 2375-2398, 2006.

[79] S. M. Spearing and A. G. Evans, "The role of fiber bridging in the delamination resistance of fiber-reinforced composites," *Acta Metallurgica et Materialia,* vol. 40, pp. 2191-2199, 1992.

[80] J. N. Sultan and F. J. McGarry, "Effect of rubber particle size on deformation mechanisms in glassy epoxy," *Polymer Engineering & Science,* vol. 13, pp. 29-34, 1973.

[81] D. C. Marcano, D. V. Kosynkin, J. M. Berlin, A. Sinitskii, Z. Sun, A. Slesarev, L. B. Alemany, W. Lu, J. M. Tour, "Improved Synthesis of Graphene Oxide," *ACS Nano,* vol. 4, pp. 4806-4814, 2010.

[82] "Standard Test Method for Mode I Interlaminar Fracture Toughness of Unidirectional Fiber-Reinforced Polymer Matrix Composites," ed. West Conshohocken, Pennsylvania 19428-2959, United States: ASTM International, 2007, pp. 1-12.

[83] "Standard Test Methods for Flexural Properties of Unreinforced and Reinforced Plastics and Electrical Insulating Materials," ed. West Conshohocken, Pennsylvania 19428-2959, United States: ASTM International, 2010, pp. 1-11.

[84] James M. Gere, Stephen P. Timoshenko, *Mechanics of Materials*, 7 ed.

[85] Ho Peter, Lay-Lay Chua, S. Wang, Perq-jon Chia, Goh Ghim Siong, Chia Perq-jon, Goh Ghim Siong, "Functionalized Graphene Oxide," United States Patent, 2011.

[86] K. E. Smith, S. S. Parks, M. A. Hyjek, S. E.Downey, K. Gall, "The effect of the glass transition temperature on the toughness of photopolymerizable (meth)acrylate networks under physiological conditions," *Polymer,* vol. 50, pp. 5112-5123, 2009.

[87] P. R. Thakre, P. R. Thakre, D. C. Lagoudas, J. C. Riddick, T. S. Gates, Sarah-Jane V. Frankland, J. G. Ratcliffe, J. Zhu,E. V. Barrera, "Investigation of the effect of single wall carbon nanotubes on interlaminar fracture toughness of woven carbon fiber-epoxy composites," *Journal of Composite Materials,* March 8, 2011 2011.

[88] M. Hussain, A. Nakahira, S. Nishijima, K. Niihara, "Fracture behavior and fracture toughness of particulate filled epoxy composites," *Materials Letters,* vol. 27, pp. 21-25, 1996.

[89] J. Han and K. Cho, "Nanoparticle-induced enhancement in fracture toughness of highly loaded epoxy composites over a wide temperature range," *Journal of Materials Science,* vol. 41, pp. 4239-4245, 2006.

[90] B. Partoens and F. M. Peeters, "From graphene to graphite: Electronic structure around the K point," *Physical Review B,* vol. 74, p. 075404, 2006.

[91] W. H. Lu, F. S. Liao, A. C. Su, P. W. Kao, T. J. Hsu, "Effect of interleaving on the impact response of a unidirectional carbon/epoxy composite," *Composites,* vol. 26, pp. 215-222, 1995.

[92] T. Yokozeki, Y. Iwahori, S. Ishiwata, K. Enomoto, "Mechanical properties of CFRP laminates manufactured from unidirectional prepregs using CSCNT-dispersed epoxy," *Composites Part A: Applied Science and Manufacturing,* vol. 38, pp. 2121-2130, 2007.

[93] J. Zhang and C. He, "A three-phase cylindrical shear-lag model for carbon nanotube composites," *Acta Mechanica,* vol. 196, pp. 33-54, 2008.

VITA

SESHASAI GANDIKOTA

Candidate for the Degree of

Master of Science

Thesis: SELECTIVE TOUGHENING OF CARBON/EPOXY COMPOSITES USING GRAPHENE OXIDE

Major Field: Mechanical and Aerospace Engineering

Biographical:

Education:

Received Bachelor of Science Degree in Mechanical Engineering at Osmania University, India in 2008.

Completed the requirements for the Master of Science in your major at Oklahoma State University, Stillwater, Oklahoma in July, 2011.

Experience:

Worked as a Graduate Research Assistant for Dr. Ranji Vaidyanathan in polymer nanocomposites.

Name: Seshasai Gandikota Date of Degree: December, 2011

Institution: Oklahoma State University Location: Stillwater, Oklahoma

Title of Study: SELECTIVE TOUGHENING OF CARBON/EPOXY COMPOSITES USING GRAPHENE OXIDE

Pages in Study: 73 Candidate for the Degree of Master of Science

Major Field: Mechanical and Aerospace Engineering

Scope and Method of Study:

The study presented in the thesis suggests a method of incorporating graphene oxide nanofillers into carbon fiber reinforced epoxy composites. The method uses nano-reinforcement in the interlaminar region of the composites, thereby reducing the material cost and increasing the ease of processing.

Findings and Conclusions:

A 100 % improvement in the fracture toughness of the composites has been achieved without sacrificing the flexural properties.

Use of graphene oxide fillers is reported and an efficient method of incorporating them into fiber reinforced epoxy composites is demonstrated.

ADVISER'S APPROVAL: Jay C Hanan